Published online September 8, 2004

4786–4803 *Nucleic Acids Research, 2004, Vol. 32, No. 16*
doi:10.1093/nar/gkh783

Portrait of transcriptional responses to ultraviolet and ionizing radiation in human cells

Kerri E. Rieger and Gilbert Chu*

Department of Medicine and Department of Biochemistry, Stanford University School of Medicine, Stanford, CA 94305, USA

Received May 27, 2004; Revised and Accepted August 3, 2004

ABSTRACT

To understand the human response to DNA damage, we used microarrays to measure transcriptional responses of 10 000 genes to ionizing radiation (IR) and ultraviolet radiation (UV). To identify bona fide responses, we used cell lines from 15 individuals and a rigorous statistical method, Significance Analysis of Microarrays (SAM). By exploring how sample number affects SAM, we rendered a portrait of the human damage response with a degree of accuracy unmatched by previous studies. By showing how SAM can be used to estimate the total number of responsive genes, we discovered that 24% of all genes respond to IR and 32% respond to UV, although most responses were less than 2-fold. Many genes were involved in known damage-response pathways for cell cycling and proliferation, apoptosis, DNA repair or the stress response. However, the majority of genes were involved in unexpected pathways, with functions in signal transduction, RNA binding and editing, protein synthesis and degradation, energy metabolism, metabolism of macromolecular precursors, cell structure and adhesion, vesicle transport, or lysosomal metabolism. Although these functions were not previously associated with the damage response in mammals, many were conserved in yeast. These insights reveal new directions for studying the human response to DNA damage.

INTRODUCTION

DNA is vulnerable to the onslaught of a wide variety of DNA damaging agents. Ultraviolet radiation (UV) and ionizing radiation (IR) produce lesions that are representative of many other agents. UV from the sun produces oxidized bases, single-strand breaks and intrastrand cross-links in the form of cyclobutane pyrimidine dimers and (6-4) photoproducts. IR has many sources, including radon decay from the soil and X-rays from medical practice, and induces oxidized bases and breaks in one or both strands of DNA.

UV and IR elicit complex cellular responses involving several signaling pathways (1). Although some proteins are regulated post-transcriptionally, many are regulated at the level of gene transcription. Transcriptional responses to DNA damage have not been well characterized in mammalian cells. Only about 100 damage-inducible transcripts were identified using methods such as subtractive hybridization or differential display [reviewed in (2,3)]. Because microarrays can measure the transcriptional levels of thousands of genes simultaneously, several groups have used microarrays to study the damage response. Responses in yeast (4–7) and *Escherichia coli* (8) have been reported. Although many features of the damage response are conserved from micro-organisms to humans (9,10), the response in humans will have features not found in yeast or *E.coli*.

Microarray analyses of the damage response in human cells have been limited by small numbers of samples. The vast datasets generated by microarray experiments must be replicated to ensure statistical validity. Some studies have used only duplicates (11) or no replicates at all (12). Other studies have included replicates from only one cell line (13–15) or cells from only one donor (12), thus failing to account for variation among individuals.

In addition, some studies have employed flawed methods of gene selection. For example, some studies (11,16–18) considered a gene significantly induced or repressed if an R-fold change was observed, where R is the ratio of gene expression between two states. This approach does not account for the variation in expression across samples and selects a high percentage of genes with apparent changes in expression that are not statistically significant (19). Moreover, these analyses are biased toward the detection of highly induced mRNAs. Other studies (15) have accounted for sample variability by utilizing t-tests, but failed to address the problem of multiple hypothesis testing. This problem is particularly vexing when transcriptional responses of thousands of genes are measured simultaneously, because a simple t-test with an apparently stringent requirement such as $P < 0.01$ will identify hundreds of genes by chance (19).

To obtain a genome-wide portrait of the transcriptional response to DNA damage in human cells, we used oligonucleotide microarrays to measure the responses of 10 000 genes in cell lines from 15 different individuals. The 15 cell lines served as replicates and allowed us to identify responses that were independent of variations among different individuals. We analyzed the data using a statistically rigorous method, Significance Analysis of Microarrays (SAM), which provided

*To whom correspondence should be addressed at CCSR 1145, Division of Oncology, Stanford University Medical Center, Stanford, CA 94305-5151, USA. Tel: +1 650 725 6442; Fax: +1 650 736 2282; Email: chu@cmgm.stanford.edu

an estimate of the false discovery rate (FDR) for responsive genes (19). To better describe the transcriptional responses to DNA damage, we utilized novel applications of SAM. We systematically explored how sample number affects the FDR in SAM, and demonstrated that cell lines from 15 different individuals provide an accurate portrait of the transcriptional response to DNA damage. We showed how SAM could be applied to estimate the total number of genes in the genome that respond to DNA damage. Our data permitted us to identify a large number of genes with unprecedented confidence. Several approaches confirmed that our portrait of transcriptional responses was reproducible and accurate. Surprisingly, a majority of the responsive genes proved to be unanticipated.

MATERIALS AND METHODS

Cell lines

Fifteen healthy individuals, ages 21–36, were recruited in accordance with Stanford regulations for human subjects research. The data were originally collected as controls for a study of transcriptional responses in patients with toxicity from radiation therapy (20). Lymphoblastoid cell lines were established by immortalization of peripheral blood B-lymphocytes with Epstein–Barr virus from the B95-8 monkey cell line. The cells were grown in RPMI 1640 (Gibco) with 15% heat-inactivated fetal bovine serum, 1% penicillin/streptomycin and 2 mM glutamine, and stored in liquid nitrogen.

Treatment of cells with UV and IR

Lymphoblastoid cells were thawed and grown to generate 10^8 cells. The cells were divided into three aliquots for mock, UV and IR treatment. For UV treatment, 5×10^7 cells were suspended in phosphate-buffered saline (PBS) at 6×10^5 cells/ml to ensure uniform exposure to UV. Aliquots designated for mock treatment and IR treatment were also suspended in PBS during this period to ensure similar treatment. The cells were UV irradiated for 15 s with a germicidal lamp (254 nm) at a fluence of 0.67 J/m^2/s to a dose of 10 J/m^2, seeded at 3×10^5 cells/ml in fresh media and harvested for RNA 24 h later. For treatment with IR, 4×10^7 cells were exposed to 5 Gy IR 20 h after the PBS wash and harvested for RNA 4 h later together with the UV-treated samples.

Microarray hybridization

RNA was labeled with biotin and hybridized to a U95A_v2 GeneChip® microarray, according to the manufacturer's protocols (Affymetrix, Santa Clara, CA). This microarray contains 12 625 probe sets representing ~10 000 genes. The expression level for each gene was calculated by Affymetrix GeneChip Microarray Analysis Suite software version 4.0. To account for differences in hybridization between different chips, data from hybridizations were scaled to the average of all datasets, as described (19). The complete dataset is available at http://www.ncbi.nlm.nih.gov/geo/.

Analysis of microarray data

We used the paired data option in SAM (19) to identify the UV and IR response genes. (The Excel plug-in software is available at http://www-stat.stanford.edu/~tibs/SAM/.) The input for this analysis included the mock-treatment versus IR-treatment data to identify the IR-responsive genes, and mock-treatment versus UV-treatment data to identify the UV-responsive genes. Hierarchical clustering (21) used uncentered Pearson correlation and complete linkage clustering, and was displayed using TreeView (http://rana.lbl.gov/EisenSoftware.htm). Biological functions were assigned from published literature, Locus Link (http://www.ncbi.nlm.nih.gov/LocusLink/), and the SOURCE database (http://source.stanford.edu).

RESULTS

Estimate of accuracy in identifying damage-response genes

Because microarray studies probe the entire genome, they often identify genes with surprising functions. Such genes could represent either novel observations or experimental errors. To address this issue, we conducted experiments to ensure that our identification of damage-response genes would be highly accurate. This section describes the results of those experiments.

We established lymphoblastoid cell lines from 15 healthy individuals, 14 of European and 1 of Hispanic descent, and collected RNA from cells 4 h after exposure to 5 Gy IR and 24 h after exposure to 10 J/m^2 UV. The time intervals were based on previous reports showing maximal response to IR (22) or UV (23) at 4 and 24 h, respectively. The UV response is known to be more gradual than the IR response. Cell viability was 97% at 4 h post-IR and 90% at 24 h post-UV by trypan blue exclusion, compared to 98% in mock-treated cells.

It is important to note that the IR and UV responses measured in our experiments reflect changes in transcript levels, which are not necessarily due to the changes in rates of transcription. Indeed, altered transcript levels may also be due to the changes in rates of transcript degradation. For example, UV exposure induces stabilization of c-fos mRNA and other short-lived mRNAs (24). Our experiments were conducted without inhibiting protein synthesis. Therefore, responses identified in this study include secondary responses, which help to complete the portrait of transcriptional responses. For example, DNA damage induces cell cycle arrest, and many responses in genes involved in cell cycle or proliferation may reflect the altered distribution of cells in the cell cycle following radiation.

We used oligonucleotide microarrays containing 12 625 probe sets to measure the responses in gene expression levels after UV or IR. In some cases, several probe sets corresponded to the same gene, so that the microarrays measured the expression of ~10 000 genes. The data were analyzed with SAM, which assigns a relative difference, $d(i)$, for each gene i based on the change in gene expression relative to the standard deviation (SD) of repeated measurements for gene i. Genes with $d(i)$ values satisfying an adjustable threshold parameter Δ are called potentially significant. The FDR is the percentage of such genes identified by chance. SAM calculates the FDR by randomly permuting the sample labels and counting the number of genes with $d(i)$ values satisfying the threshold parameter Δ.

An experiment by Tusher *et al*. (19) from our laboratory previously used SAM to measure the effect of IR on gene

expression. To determine whether SAM provides an accurate estimate of the FDR, we used data from the current study with 15 individuals to verify the results from Tusher *et al*. Using SAM, Tusher *et al*. identified 36 probe sets that changed at least 1.5-fold with an FDR of 12%. Two of the thirty-six probe sets were not on the array in the current study. Of the 34 remaining probe sets, 28 (82.4%) were ranked as highly significant in the current study, since they were among the set of top-ranked genes identified by SAM with an FDR of 1.5%. Thus, the FDR provided by SAM in the Tusher *et al*. study is supported by the current study.

Tusher *et al*. (19) also tested the validity of SAM by performing northern blots for 20 genes and found a good correlation of the northern blot results with expression of the genes highly ranked by SAM. We compared our microarray results to northern-blot results from Tusher *et al*. (Figure 1) and found an even stronger correlation.

In microarray experiments, increased statistical power from a large number of samples must be balanced against the cost of the microarrays. The effect of sample size on the number of significantly changing genes identified by SAM is thus a critical issue, and has not been addressed previously. We explored how the number of samples influenced the FDR for different numbers of probe sets called significant (Figure 2). We used SAM to search for IR-responsive probe sets, generating an FDR curve for different sets of cell lines, including three non-overlapping sets of 2 samples, three non-overlapping sets of 4 samples, two non-overlapping sets of 7 samples, a set of 10 samples and a set of 15 samples.

Increasing the number of samples increased the stability of the FDR (Figure 2). The three sets of 2 samples (2a, 2b and 2c) produced widely divergent FDR curves, while the three sets of 4 samples (4a, 4b and 4c) produced more reproducible FDR curves. Finally, the FDR curves were nearly super-imposable for the two sets of 7 samples (7a and 7b). For the smaller sample sets, the wide divergence in FDR may be due to several factors: inaccurate estimation of experimental error due to the small number of measurements, variations in the human population and the smaller number of permutations available for estimating the true FDR. These problems become less important as the number of samples increases.

Decreasing the threshold parameter Δ increases the number of genes called significant (19), but at the cost of a higher FDR (Figure 2). Increasing the number of samples permitted identification of an increased number of IR-responsive probe sets for a given FDR. For an FDR of 10%, SAM identified only 110 probe sets from a set of 4 samples, 700 probe sets from a set of 7 samples, 1270 probe sets from a set of 10 samples and nearly 2000 IR-responsive probe sets from a set of 15 samples.

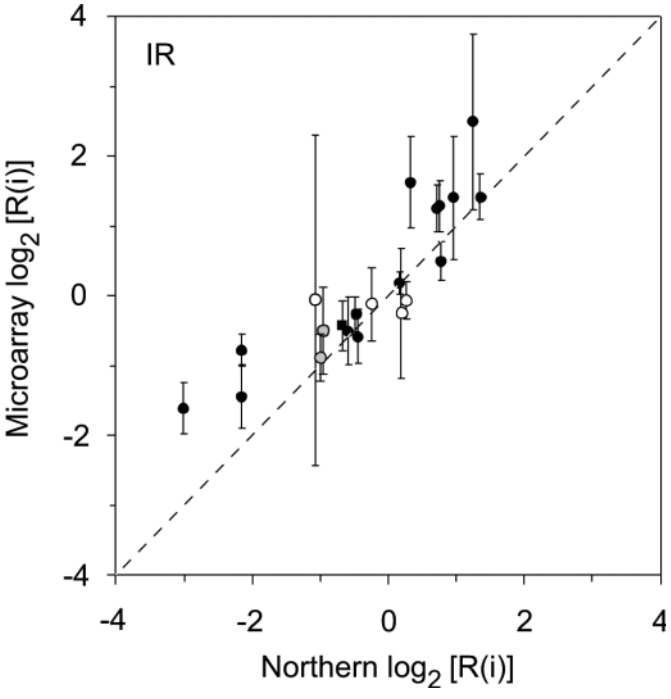

Figure 1. Correlation between northern blots and microarray measurements of gene expression. The logarithms of fold-changes $R(i)$ from northern blots for 20 genes were plotted against the logarithms of fold-changes from the microarray measurements in the current study. The northern-blot data were obtained from Tusher *et al*. (19). The logarithms of fold-changes from microarray data were obtained by averaging the logarithms of the pairwise fold-changes for all 15 samples. The error flags indicate the SD of the logarithms of the pairwise fold-changes for the 15 samples. Fifteen of the twenty-one (71%) genes plotted had SDs that crossed the line of identity $x = y$. Four of the genes had low ranks by SAM associated with FDR > 50% (open circles). The squared correlation coefficient $R^2 = 0.823$ was obtained using the remaining genes, which were contained in the set of genes with FDR < 10%. One gene (cyclin F) is represented by two probe sets on the microarray, and values for both probe sets are plotted (gray circles). One gene was analyzed by quantitative PCR (closed square).

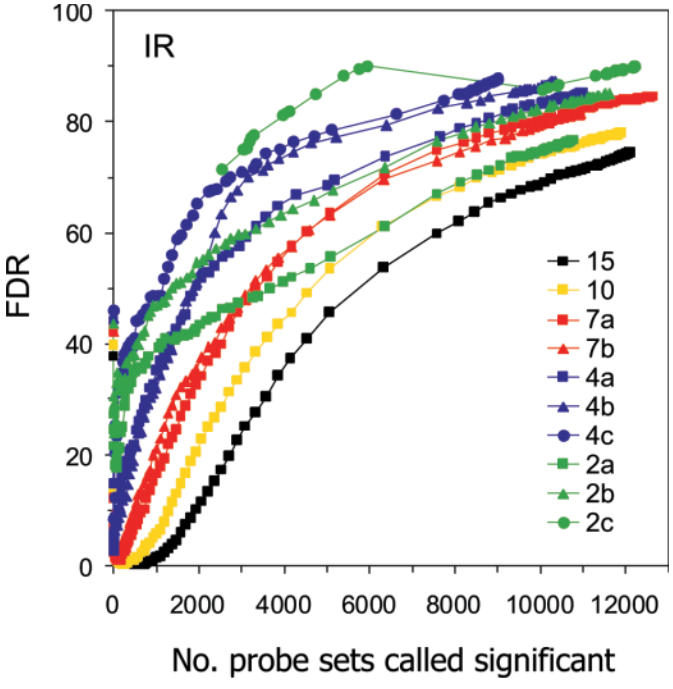

Figure 2. Effect of number of samples on FDR. SAM was used to identify probe sets responsive to IR. The graph shows curves of FDR (expressed as a percentage) as a function of the number of probe sets called significantly changing. Each curve was generated for a given set of samples from 2, 4, 7, 10 or 15 individuals. The sets containing 2, 4 and 7 samples were non-overlapping. For example, set 7a included seven samples (1–7), and set 7b included seven different samples (8–14). Increasing the number of samples led to a dramatic decrease and stabilization in the FDR. Note that SAM sometimes generated anomalously high values for FDR when the number of probe sets called significant was small.

Increasing the number of samples even further would result in a further increase in the number of responsive genes identified by SAM.

IR and UV affect the expression of thousands of genes

Microarray analysis is capable of determining the total number of differentially expressed genes. In particular, SAM can estimate the probability ($1 - \pi_0$) that a probe set has responded transcriptionally to IR or UV [(25); http://www-stat.stanford.edu/~tibs/SAM/]. The estimate for $1 - \pi_0$ by SAM indicated that 24% of genes were IR-responsive and 32% of the genes were UV-responsive. The actual percentage of induced genes may even be slightly higher, since the FDR would be expected to decrease slightly if the number of replicates increases beyond 15 (Figure 2).

To display these estimates graphically, we noted that the net number of responding probe sets is equal to the number of probe sets called significant multiplied by (1 − FDR). When we plotted the net number of responding probe sets versus the number of probe sets called significant, the curve for either IR-responsive or UV-responsive genes rapidly approached an asymptotic value and remained constant over a wide range (Figure 3). The total number of responsive probe sets in our microarray experiments was $12\,625 \times (1 - \pi_0)$, which was equal to 3030 IR-responsive probe sets and 4040 UV-responsive probe sets. These values closely matched the asymptotic values in the plotted data.

The rapid asymptotic behavior of the curves meant that about half of all responsive genes could be identified with an FDR of only 10%. For an FDR of 10%, SAM identified 1932 IR-responsive probe sets and 3143 UV-responsive probe sets, which are listed in Supplementary Material Tables 1 and 2. A total of 1111 of these probe sets responded to both UV and IR.

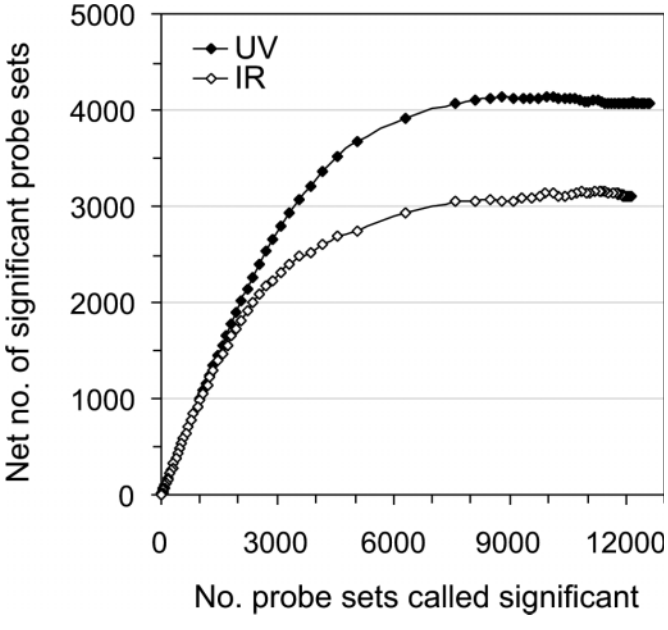

Figure 3. Estimate of total number of differentially expressed probe sets. The net number of significant probe sets was plotted as a function of the FDR from an analysis by SAM of all 15 samples. The net number of significant probe sets is the number called significant multiplied by (1−FDR). The net number reached an asymptotic value, providing an estimate of the total number of damage-responsive probe sets.

Fold-changes of differentially expressed genes

We examined the magnitude of the changes in the expression for the IR- and UV-responsive genes (Figure 4). The great majority of genes called significant with an FDR of 10% changed 1.1–1.5-fold. The histogram showed a dip for genes changing less than 1.1-fold because these changes were usually small relative to the SD of repeated measurements. The $d(i)$ for most of these genes had a small value, and the changes in expression were thus statistically insignificant.

Many microarray studies have attempted to identify genes responding to IR or UV by using the fold-change method. In this method, genes are deemed responsive if their expression changes by 2-fold or even higher (11,16–18). In our study, a 2-fold cutoff would have eliminated 93 and 95% of the genes responding to UV and IR, respectively. In contrast, SAM can identify subtle but statistically significant changes in gene expression.

Identity of damage-responsive genes

To identify genes with statistically significant responses to IR or UV that also have the potential for being biologically meaningful, we applied SAM in conjunction with a 1.3-fold change cutoff. Of course, the choice of a 1.3-fold cutoff is somewhat arbitrary. We could have chosen a more stringent cutoff, but this would have eliminated responses that may prove to be meaningful. For example, the combined responses of a group of genes acting in concert might affect the physiology of the cell, even if each change is less than 2-fold. Indeed, the results discussed below include several sets of genes that can be grouped together in biochemical pathways.

Among genes changing at least 1.3-fold, a total of 526 IR-responsive and 1113 UV-responsive probe sets were associated with an FDR of 10%. The top-ranked 200 IR-responsive probe sets (Table 1) and 200 UV-responsive probe sets (Table 2) were associated with FDRs <0.4%. Many were previously known to be IR- or UV-responsive, providing further validation of our results. Because genes were often represented by multiple probe sets on the microarray, several top-ranked genes appeared more than once. For example, four of the six probe sets for *TNFRSF6* on the microarray were among the top 200 IR-responsive probe sets identified by SAM (Table 1).

We categorized the top-ranked damage-responsive genes by function (Figure 5). These genes are discussed in the following section, and a more extensive description is available in Supplementary Material Appendix 1. The IR- and UV-responsive genes had similar distributions among the functional categories. Indeed, 50 probe sets were among the 200 top-ranked probe sets for both IR and UV responses. Interestingly, only 41% of the IR- and UV-responsive genes had functions in the cell cycle and proliferation, apoptosis, DNA repair or the stress response, which are functions previously associated with the DNA damage response. The remaining 59% of genes had functions that have not been well studied in the context of the damage response.

Table 1. Highest ranked IR-responsive genes

Accession no.	Symbol; Name	*R*(*i*)
Cell cycle/proliferation		
AF059617	SNK; serum-inducible kinase	(+) 7.3
U03106	CDKN1A; cyclin-dependent kinase inhibitor 1A (p21)	(+) 4.2
AI038821	HRAS; Harvey rat sarcoma viral oncogene hom.	(+) 2.4
AA586695	PVT1; pvt-1 (murine) oncogene hom., MYC activator	(+) 2.3
D38305	TOB1; transducer of ERBB2, 1	(+) 1.8
X77794	CCNG1; cyclin G1	(+) 1.7
J00277	HRAS; v-Ha-ras Harvey rat sarcoma viral oncogene hom.	(+) 1.7
AA586695	PVT1; pvt-1 (murine) oncogene hom., MYC activator	(+) 1.6
U56998	CNK; cytokine-inducible kinase	(+) 1.5
U48296	PTP4A1; protein tyrosine phosphatase type IVA, 1	(+) 1.4
U88629	ELL2; ELL-related RNA polymerase II, elongation factor	(+) 1.3
X61123	BTG1; B-cell translocation gene 1, anti-proliferative	(+) 1.3
D88435	GAK; cyclin G associated kinase	(+) 1.3
U72649	BTG2; BTG family, member 2	(+) 1.3
AF055008	GRN; granulin	(+) 1.3
U17105	CCNF; cyclin F	(−) 29.8
Z15005	CENPE; centromere protein E (312 kDa)	(−) 3.3
U05340	CDC20; CDC20 cell division cycle 20 hom. (yeast)	(−) 3.2
AF011468	STK6; serine/threonine kinase 6	(−) 3.1
U01038	PLK; polo-like kinase	(−) 3.0
AF011468	STK6; serine/threonine kinase 6	(−) 2.8
X67155	KNSL5; kinesin-like 5 (mitotic kinesin-like protein 1)	(−) 2.8
M25753	CCNB1; cyclin B1	(−) 2.7
M25753	CCNB1; cyclin B1	(−) 2.6
U14518	CENPA; centromere protein A (17 kDa)	(−) 2.5
V00568	MYC; v-myc avian myelocytomatosis viral oncogene hom.	(−) 2.3
D13633	DLG7; discs, large hom. 7 (*Drosophila*)	(−) 2.1
D26361	KIF14; kinesin family member 14	(−) 2.1
AF053305	BUB1; budding uninhibited by benzimidazoles 1 (yeast)	(−) 2.0
AB024704	C20orf1; chromosome 20 open reading frame 1	(−) 2.0
Z29066	NEK2; NIMA (never in mitosis gene a)-related kinase 2	(−) 1.9
U30872	CENPF; centromere protein F (350/400 kDa, mitosin)	(−) 1.9
AL080146	CCNB2; cyclin B2	(−) 1.8
Z36714	CCNF; cyclin F	(−) 1.8
AF053306	BUB1B; budding uninhibited by benzimidazoles 1 (yeast) β	(−) 1.7
X54942	CKS2; CDC28 protein kinase 2	(−) 1.7
V00568	MYC; v-myc myelocytomatosis viral oncogene hom.	(−) 1.7
D14678	KNSL2; kinesin-like 2	(−) 1.6
X51688	CCNA2; cyclin A2	(−) 1.6
X65550	MKI67; antigen for monoclonal antibody Ki-67	(−) 1.6
X65550	MKI67; antigen for monoclonal antibody Ki-67	(−) 1.5
AL031588	GTSE1; G_2 and S-phase expressed 1	(−) 1.5
U63743	KNSL6; kinesin-like 6 (mitotic centromere-associated kinesin)	(−) 1.5
X51688	CCNA2; cyclin A2	(−) 1.5
AF017790	HEC; highly expressed in cancer	(−) 1.5
U37426	KNSL1; kinesin-like 1	(−) 1.5
AF063308	SPAG5; sperm-associated antigen 5	(−) 1.5
L25876	CDKN3; cyclin-dependent kinase inhibitor 3	(−) 1.5
X82260	RANGAP1; Ran GTPase activating protein 1	(−) 1.5
M86699	TTK; TTK protein kinase	(−) 1.4
AF015254	STK12; serine/threonine kinase 12 (aurora-1)	(−) 1.4
AI375913	TOP2A; topoisomerase (DNA) II α (170 kDa)	(−) 1.4
AB028069	ASK; activator of S phase kinase	(−) 1.4
AB005754	POLS; polymerase (DNA-directed) σ	(−) 1.3
M21154	AMD1; *S*-adenosylmethionine decarboxylase 1	(−) 1.3
Apoptosis		
AB000584	PLAB; prostate differentiation factor (ptgf-β)	(+) 4.9
U29332	FHL2; four and a half LIM domains 2	(+) 3.1
U03398	TNFSF9; TNF (ligand) superfamily, member 9	(+) 2.6
X63717	TNFRSF6; TNF receptor superfamily, member 6	(+) 2.6
Z70519	TNFRSF6; TNF receptor superfamily, member 6	(+) 2.4
X83492	TNFRSF6; TNF receptor superfamily, member 6	(+) 2.4
X83490	TNFRSF6; TNF receptor superfamily, member 6	(+) 2.4
AF016266	TNFRSF10B; TNF receptor superfamily, member 10b	(+) 2.3
L08096	TNFSF7; TNF (ligand) superfamily, member 7	(+) 2.1
X89101	TNFRSF6; TNF receptor superfamily, member 6	(+) 2.0
U19599	BAX; BCL2-associated X protein	(+) 1.9
AF010313	PIG8; etoposide-induced mRNA	(+) 1.9
U48705	DDR1; discoidin domain receptor family, member 1	(+) 1.8

Table 1. *Continued*

Accession no.	Symbol; Name	*R*(*i*)
L22473	BAX; BCL2-associated X protein	(+) 1.8
D90070	PMAIP1; phorbol-12-myristate-13-acetate-induced	(+) 1.6
U59863	TANK; TRAF family-associated NFκB activator	(+) 1.5
X86809	PEA15; phosphoprotein enriched in astrocytes 15	(+) 1.4
X80200	TRAF4; TNF receptor-associated factor 4	(+) 1.4
DNA repair		
M60974	GADD45A; growth arrest and DNA-damage-inducible α	(+) 4.1
D21089	XPC; xeroderma pigmentosum complementation group C	(+) 3.1
U18300	DDB2; damage-specific DNA binding protein 2 (48 kDa)	(+) 2.4
J05614	PCNA; proliferating cell nuclear antigen	(+) 2.2
M15796	PCNA; proliferating cell nuclear antigen	(+) 1.9
M36067	LIG1; ligase I, DNA, ATP-dependent	(+) 1.8
AF029669	RAD51C; RAD51 hom. C (*S.cerevisiae*)	(+) 1.5
AF029670	RAD51C; RAD51 hom. C (*S.cerevisiae*)	(+) 1.4
AL096744	REV3L; REV3-like (yeast), DNA pol ζ catalytic subunit	(+) 1.4
Stress response		
L19871	ATF3; activating transcription factor 3	(+) 2.9
AF010309	PIG3; quinone oxidoreductase hom.	(+) 2.8
U78305	PPM1D; protein phosphatase 1D magnesium-dependent	(+) 2.4
AB007455	TP53TG1; TP53 target gene 1	(+) 2.3
M83221	RELB; v-rel reticuloendotheliosis viral oncogene hom. B	(+) 1.5
S76638	NFkB2; nuclear factor for κ light chain enhancer in B-cells 2	(+) 1.5
S76638	NFkB2; nuclear factor for κ light chain enhancer in B-cells 2	(+) 1.4
X13710	GPX1; glutathione peroxidase 1	(+) 1.3
L29277	STAT3; signal transducer and activator of transcription 3	(+) 1.3
M62831	ETR101; immediate early protein	(−) 1.6
L08895	MEF2C; MADS box transcription enhancer factor 2C	(−) 1.4
U12779	MAPKAPK2; MAP kinase-activated protein kinase 2	(−) 1.3
Signal transduction		
L08488	INPP1; inositol polyphosphate-1-phosphatase	(+) 2.8
X85545	PRKX; protein kinase, X-linked	(+) 1.9
U70426	RGS16; regulator of G-protein signaling 16	(+) 1.9
L20971	PDE4B; phosphodiesterase 4B, cAMP-specific	(+) 1.6
U81802	PIK4CB; phosphatidylinositol 4-kinase, catalytic β polypeptide	(+) 1.5
AI263885	WSX-1; class I cytokine receptor	(+) 1.5
L31584	CCR7; chemokine (C–C motif) receptor 7	(+) 1.5
U94905	DGKZ; diacylglycerol kinase, ζ (104 kDa)	(+) 1.4
AF001846	PTPN22; protein tyrosine phosphatase, non-receptor type 22	(+) 1.4
AJ001902	TRIP6; thyroid hormone receptor interactor 6	(+) 1.4
AB000520	APS; adaptor protein with PH and SH2 domains	(−) 1.7
U26710	CBLB; Cas-Br-M (murine) ectropic retroviral transforming sequence b	(−) 1.6
X91809	RGS19; regulator of G-protein signaling 19	(−) 1.5
L15388	GPRK5; G-protein-coupled receptor kinase 5	(−) 1.5
AB005047	SH3BP5; SH3-domain binding protein 5 (BTK-associated)	(−) 1.4
RNA binding/editing		
AJ223948	RNAH; RNA helicase family	(+) 1.9
AA806768	APOBEC3C; apolipoprotein B mRNA editing, catalytic subunit	(+) 1.5
AL078641	APOBEC3G; apolipoprotein B mRNA editing, catalytic subunit	(+) 1.5
AL022318	APOBEC3C; apolipoprotein B mRNA editing, catalytic subunit	(+) 1.4
AF080561	RBM14; RNA binding motif protein 14	(+) 1.4
U15782	CSTF3; cleavage stimulation factor 3 for 3′ pre-RNA	(+) 1.4
Protein synthesis/degradation		
U39400	MRPL49; mitochondrial ribosomal protein L49	(+) 1.7
U73379	UBE2C; ubiquitin-conjugating enzyme E2C	(−) 1.9
M91670	E2-EPF; ubiquitin carrier protein	(−) 1.8
M91670	E2-EPF; ubiquitin carrier protein	(−) 1.7
M91670	E2-EPF; ubiquitin carrier protein	(−) 1.7
D25218	RRS1; ribosome biogenesis regulatory protein (yeast)	(−) 1.4
D78514	UBE2G1; ubiquitin-conjugating enzyme E2G 1	(−) 1.4
AI701164	UBE2G1; ubiquitin-conjugating enzyme E2G 1	(−) 1.4
Energy metabolism		
J03826	FDXR; ferredoxin reductase	(+) 2.3
L29254	SORD; sorbitol dehydrogenase	(+) 1.4
X04011	CYBB; cytochrome *b*-245, β polypeptide	(−) 1.5
Metabolism of macromolecular precursors		
AF022116	PRKAB1; protein kinase, AMP-activated β1 non-catalytic subunit	(+) 2.3
U19523	GCH1; GTP cyclohydrolase 1	(+) 1.7
U47101	NIFU; nitrogen fixation cluster-like	(+) 1.5
X02308	TYMS; thymidylate synthetase	(+) 1.4

Table 1. *Continued*

Accession no.	Symbol; Name	*R*(*i*)
D00596	TYMS; thymidylate synthetase	(+) 1.4
L00352	LDLR; low-density lipoprotein receptor	(−) 1.5
AF035284	FADS1; fatty acid desaturase 1	(−) 1.3
Cell structure/adhesion		
AB002313	PLXNB2; plexin B2	(+) 2.6
U97519	PODXL; podocalyxin-like	(+) 2.4
X13839	ACTA2; actin α2, smooth muscle, aorta	(+) 2.1
AF062341	CTNND1; catenin (cadherin-associated protein) δ1	(+) 1.8
M13452	LMNA; lamin A/C	(+) 1.7
M24283	ICAM1; intercellular adhesion molecule 1 (CD54)	(+) 1.4
AJ238764	GNE; UDP-GlcNAc 2-epimerase/*N*-acetylmannosamine kinase	(+) 1.3
Y10183	ALCAM; activated leucocyte cell adhesion molecule	(+) 1.3
X16983	ITGA4; integrin α4	(−) 1.9
AB002311	PDZ-GEF1; PDZ domain containing GEF1	(−) 1.5
L25931	LBR; lamin B receptor	(−) 1.4
AL021707	UNC84B; unc-84 hom. B (*Caenorhabditis elegans*)	(−) 1.4
Miscellaneous		
AL050276	ZNF288; zinc finger protein 288	(+) 2.3
AB013924	LAMP3; lysosomal-associated membrane protein 3	(+) 2.0
AF031815	KCNN3; K+ intermediate/small conductance Ca-activated channel	(+) 1.9
M29877	FUCA1; fucosidase, α-L- 1, tissue	(+) 1.8
D87449	UGTREL7; UDP-glucuronic acid/UDP-GalNAc transporter	(+) 1.7
Y08200	RABGGTA; Rab geranylgeranyltransferase, α subunit	(+) 1.6
D87432	SLC7A6; solute carrier family 7 (cationic amino acid transporter)	(+) 1.6
J03040	SPARC; secreted protein, acidic, cysteine-rich	(+) 1.6
AF016903	AGRN; agrin	(+) 1.6
AF038202	STX6; syntaxin 6	(+) 1.5
L06175	P5-1; MHC class I region ORF	(+) 1.5
X62078	GM2A; GM2 ganglioside activator protein	(+) 1.5
AI133727	ZAP; ZAP: zinc finger antiviral protein	(+) 1.4
AL021154	ID3; inhibitor of DNA binding 3	(+) 1.4
AB018328	ALTE; Ac-like transposable element	(+) 1.4
X85116	EPB72; erythrocyte membrane protein band 7.2	(+) 1.3
AF032862	HMMR; hyaluronan-mediated motility receptor	(−) 2.2
U28386	KPNA2; karyopherin α 2 (RAG cohort 1, importin a 1)	(−) 1.6
D67029	SEC14L1; SEC14-like 1 (*S.cerevisiae*)	(−) 1.6
S57212	MYEF2; myocyte enhancer-binding factor 2	(−) 1.6
AL096880	ZNF278; zinc finger protein 278	(−) 1.5
U08989	SLC1A1; solute carrier family 1 (glutamate transporter)	(−) 1.5
Z46606	SMARCA3; SWI/SNF related chromatin regulator	(−) 1.5
AJ133133	ENTPD1; ectonucleoside triphosphate diphosphohydrolase	(−) 1.4
S73885	TFAP4; transcription factor AP-4	(−) 1.4
AF000416	EXTL2; exostoses (multiple)-like 2	(−) 1.4
X14850	H2AFX; H2A histone family, member X	(−) 1.4
X63469	GTF2E2; general TF IIE polypeptide 2 (β subunit, 34 kDa)	(−) 1.4
Z98744	Human DNA clone RP1-193B12 (histones, OR2B2, ESTs)	(−) 1.4
D87127	TLOC1; translocation protein 1	(−) 1.3
X97267	PTPRCAP; protein tyrosine phosphatase, C-associated protein	(−) 1.3
AF046059	CRLF3; cytokine receptor-like factor 3	(−) 1.3
M31523	TCF3; transcription factor 3 (transcription factor E2-α)	(−) 1.3
X82240	TCL1A; T-cell leukemia/lymphoma 1A	(−) 1.3
Unknown		
AB022718	DEPP; decidual protein induced by progesterone	(+) 3.2
AL021546	HSPC132; hypothetical protein HSPC132	(+) 2.9
W27419	FLJ90005; hypothetical protein FLJ90005	(+) 2.8
U79266	HSU79266; protein predicted by clone 23627	(+) 1.7
AB007879	KIAA0419; KIAA0419 gene product	(+) 1.6
AL049397	H. sapiens mRNA; cDNA from clone DKFZp586C1019	(+) 1.4
AF070539	MLF2; myeloid leukemia factor 2	(+) 1.3
AB020637	KIAA0830; KIAA0830 protein	(−) 1.6
AB002384	C6orf32; chromosome 6 open reading frame 32	(−) 1.5
AL022398	DJ434O14.5; novel putative protein similar to YIL091C yeast	(−) 1.5
D43948	KIAA0097; KIAA0097 gene product	(−) 1.5
U79256	MGC14258; hypothetical protein MGC14258	(−) 1.5
AB011178	SCOP; SCN circadian oscillatory protein	(−) 1.4
AB020630	PPP1R16B; protein phosphatase 1 regulatory subunit 16B	(−) 1.4
AF038182	LOC90355; hypothetical gene supported by AF038182	(−) 1.4
AL050102	EDFR1; erythroid differentiation-related factor 1	(−) 1.4
AW024285	FLJ12443; hypothetical protein FLJ12443	(−) 1.4
D50919	TRIM14; tripartite motif-containing 14	(−) 1.4

Table 1. *Continued*

Accession no.	Symbol; Name	*R*(*i*)
AF052162	FLJ12443; hypothetical protein FLJ12443	(−) 1.3
AL023653	CXorf9; chromosome X open reading frame 9	(−) 1.3
W28612	ESTs, similar to IgG Fc binding protein (*H.sapiens*)	(−) 1.3

Abbreviations: GEF, guanine nucleotide exchange factor; hom., homolog; TNF, tumor necrosis factor.
The 200 top-ranked probe sets by SAM with fold-changes greater than 1.3 were organized by functional category. Each gene was assigned to one category, as described in Figure 5. IR led to induction of a majority of the 200 probe sets (53%).

Table 2. Highest ranked UV-responsive genes

Accession no.	Symbol; Name	*R*(*i*)
Cell cycle/proliferation		
AF060228	RARRES3; retinoic acid receptor responder 3	(+) 2.9
U03106	CDKN1A; cyclin-dependent kinase inhibitor 1A (p21)	(+) 2.7
D38583	S100A11; S100 calcium-binding protein A11 (calgizzarin)	(+) 2.5
D38305	TOB1; transducer of ERBB2, 1	(+) 2.1
AF055008	GRN; granulin	(+) 2.0
U15932	DUSP5; dual specificity phosphatase 5	(+) 1.5
M19722	FGR; Gardner–Rasheed feline sarcoma viral oncogene hom.	(+) 1.5
X77794	CCNG1; cyclin G1	(+) 1.5
X04366	CAPN1; calpain 1, (μ/I) large subunit	(+) 1.5
AB002323	DNCH1; dynein, cytoplasmic, heavy polypeptide 1	(+) 1.5
D88435	GAK; cyclin G-associated kinase	(+) 1.4
Z35278	RUNX3; runt-related transcription factor 3	(+) 1.3
X61123	BTG1; B-cell translocation gene 1, anti-proliferative	(+) 1.3
AI986201	DNCI2; dynein, cytoplasmic, intermediate polypeptide 2	(+) 1.3
AJ223728	CDC45L; CDC45 cell division cycle 45-like (*S.cerevisiae*)	(−) 1.6
M21154	AMD1; *S*-adenosylmethionine decarboxylase 1	(−) 1.5
L23959	TFDP1; transcription factor Dp-1	(−) 1.5
U05340	CDC20; cell division cycle 20 hom. (*S.cerevisiae*)	(−) 1.5
D84557	MCM6; minichromosome maintenance deficient 6	(−) 1.5
D21262	NOLC1; nucleolar and coiled-body phosphoprotein 1	(−) 1.4
X06745	POLA; polymerase (DNA directed), α	(−) 1.4
M21154	AMD1; *S*-adenosylmethionine decarboxylase 1	(−) 1.4
M14630	PTMA; prothymosin, α (gene sequence 28)	(−) 1.4
M64231	SRM; spermidine synthase	(−) 1.4
X16277	ODC1; ornithine decarboxylase 1	(−) 1.4
M33764	ODC1; ornithine decarboxylase 1	(−) 1.4
U37022	CDK4; cyclin-dependent kinase 4	(−) 1.4
W63793	AMD1; *S*-adenosylmethionine decarboxylase 1	(−) 1.4
AF070640	POLE3; DNA polymerase ε3 (p17 subunit)	(−) 1.3
X17644	GSPT1; G_1 to S phase transition 1	(−) 1.3
L20298	CBFB; core-binding factor, β subunit	(−) 1.3
Apoptosis		
L20817	DDR1; discoidin domain receptor family, member 1	(+) 3.2
U48705	DDR1; discoidin domain receptor family, member 1	(+) 2.7
U03398	TNFSF9; TNF (ligand) superfamily, member 9	(+) 2.2
S81914	IER3; immediate early response 3	(+) 2.1
U19599	BAX; BCL2-associated X protein	(+) 1.9
X83490	TNFRSF6; TNF receptor superfamily, member 6	(+) 1.9
Z70519	TNFRSF6; TNF receptor superfamily, member 6	(+) 1.9
L22473	BAX; BCL2-associated X protein	(+) 1.8
AF016266	TNFRSF10B; TNF receptor superfamily, member 10b	(+) 1.8
X63717	TNFRSF6; TNF receptor superfamily, member 6	(+) 1.8
U45878	BIRC3; baculoviral IAP repeat-containing 3	(+) 1.7
L08096	TNFSF7; TNF (ligand) superfamily, member 7	(+) 1.7
AF010313	PIG8; etoposide-induced mRNA	(+) 1.4
U19261	TRAF1; TNF receptor-associated factor 1	(+) 1.4
X86809	PEA15; phosphoprotein enriched in astrocytes 15	(+) 1.3
X60592	TNFRSF5; TNF receptor superfamily, member 5	(+) 1.3
U33821	TAX1BP1; Tax1 binding protein 1	(+) 1.3
U84388	CRADD; Caspase and RIP adaptator with death domain	(−) 2.0
AF015767	BRE; brain and reproductive organ-expressed (TNFRSF1A modulator)	(−) 1.9

Table 2. *Continued*

Accession no.	Symbol; Name	*R*(*i*)
DNA repair		
M60974	GADD45A; growth arrest and DNA-damage-inducible α	(+) 3.6
D21089	XPC; xeroderma pigmentosum complementation group C	(+) 2.5
U18300	DDB2; damage-specific DNA binding protein 2 (48 kDa)	(+) 2.2
J05614	PCNA; proliferating cell nuclear antigen	(+) 1.5
M15796	PCNA; proliferating cell nuclear antigen	(+) 1.3
M31767	MGMT; *O*6-methylguanine-DNA methyltransferase	(−) 2.0
Stress response		
AF010309	PIG3; quinone oxidoreductase hom.	(+) 5.7
M11717	HSPA1A; heat-shock 70 kDa protein 1A	(+) 3.1
AB007455	TP53TG1; TP53 target gene 1	(+) 2.6
Z23090	HSPB1; heat-shock 27 kDa protein 1	(+) 1.8
L29277	STAT3; signal transducer and activator of transcription 3	(+) 1.6
X13710	GPX1; glutathione peroxidase 1	(+) 1.5
U70660	ATOX1; ATX1 (antioxidant protein 1, yeast) hom. 1	(+) 1.5
X61498	NFκB2; nuclear factor for κ light chain enhancer in B-cells 2	(+) 1.5
U90878	PDLIM1; PDZ and LIM domain 1 (elfin)	(+) 1.4
L29277	STAT3; signal transducer and activator of transcription 3	(+) 1.4
U51127	IRF5; interferon regulatory factor 5	(+) 1.4
X15187	TRA1; tumor rejection antigen (gp96) 1	(−) 1.5
AL022312	ATF4; activating transcription factor 4	(−) 1.4
Signal transduction		
AB002382	CTNND1; catenin (cadherin-associated protein), δ1	(+) 2.5
L31584	CCR7; chemokine (C–C motif) receptor 7	(+) 1.8
U90913	TIP-1; Tax interaction protein 1	(+) 1.8
U00672	IL10RA; interleukin 10 receptor, α	(+) 1.8
X52425	IL4R; interleukin 4 receptor	(+) 1.6
AF001846	PTPN22; protein tyrosine phosphatase, non-receptor type 22	(+) 1.6
L20971	PDE4B; phosphodiesterase 4B, cAMP-specific	(+) 1.5
X99209	HRMT1L1; HMT1 hnRNP methyltransferase-like 1	(+) 1.5
AF062075	LPXN; leupaxin	(+) 1.4
AI565760	GABARAPL2; GABA(A) receptor-associated protein-like 2	(+) 1.4
U94905	DGKZ; diacylglycerol kinase, ζ (104 kDa)	(+) 1.3
X69550	ARHGDIA; Rho GDP dissociation inhibitor (GDI) α	(−) 1.4
U96131	TRIP13; thyroid hormone receptor interactor 13	(−) 1.3
RNA binding/editing		
AA806768	APOBEC3C; apolipoprotein B mRNA editing, catalytic subunit	(+) 1.9
AL022318	APOBEC3B; apolipoprotein B mRNA editing, catalytic subunit	(+) 1.6
AL022318	APOBEC3C; apolipoprotein B mRNA editing, catalytic subunit	(+) 1.6
AL078641	APOBEC3G; apolipoprotein B mRNA editing, catalytic subunit	(+) 1.4
U41387	DDX21; DEAD/H (Asp-Glu-Ala-Asp/His) box polypeptide 21	(−) 1.6
S63912	HNRPA3; heterogeneous nuclear ribonucleoprotein A3	(−) 1.5
M65028	HNRPAB; heterogeneous nuclear ribonucleoprotein A/B	(−) 1.5
U75686	PABPC4; poly(A) binding protein, cytoplasmic 4	(−) 1.4
AF037448	NSAP1; NS1-associated protein 1	(−) 1.4
U59151	DKC1; dyskeratosis congenita 1, dyskerin	(−) 1.4
X75755	SFRS2; splicing factor, arginine/serine-rich 2	(−) 1.4
AI816034	NOLA2; nucleolar protein family A, member 2	(−) 1.4
AF054996	IMP4; U3 snoRNP protein 4 hom.	(−) 1.3
W28257	PAI-RBP1; PAI-1 mRNA-binding protein	(−) 1.3
AF039652	RNASEH1; ribonuclease H1	(−) 1.3
X75755	SFRS2; splicing factor, arginine/serine-rich 2	(−) 1.3
Protein synthesis/degradation		
U49278	UBE2V1; UEV-1 (*H.sapiens*), mRNA sequence	(+) 1.4
U46751	SQSTM1; sequestosome 1	(+) 1.3
AF097441	FARS1; phenylalanine-tRNA synthetase	(−) 2.2
D32050	AARS; alanyl-tRNA synthetase	(−) 1.4
X94754	MARS; methionine-tRNA synthetase	(−) 1.4
U89436	YARS; tyrosyl-tRNA synthetase	(−) 1.3
U04953	IARS; isoleucine-tRNA synthetase	(−) 1.3
Energy metabolism		
J03826	FDXR; ferredoxin reductase	(+) 2.7
AF030249	ECH1; enoyl coenzyme A hydratase 1, peroxisomal	(+) 1.4
X92720	PCK2; phosphoenolpyruvate carboxykinase 2	(−) 1.6
D00723	GCSH; glycine cleavage system protein H	(−) 1.5
Metabolism of macromolecular precursors		
J04430	ACP5; acid phosphatase 5, tartrate resistant	(+) 2.3
U19523	GCH1; GTP cyclohydrolase 1 (dopa-responsive dystonia)	(+) 1.9
X02994	ADA; adenosine deaminase	(+) 1.7

Table 2. *Continued*

Accession no.	Symbol; Name	*R*(*i*)
U47101	NIFU; nitrogen fixation cluster-like	(+) 1.6
U50708	BCKDHB; branched chain keto acid dehydrogenase E1β	(−) 2.5
U29344	FASN; fatty acid synthase	(−) 2.1
U50196	ADK; adenosine kinase	(−) 2.1
AB002359	PFAS; phosphoribosylformylglycinamidine synthase	(−) 1.6
U54645	AK2; adenylate kinase 2	(−) 1.5
U23143	SHMT2; serine hydroxymethyltransferase 2 (mitochondrial)	(−) 1.4
X53793	ADE2H1; similar to SAICAR synthetase and AIR carboxylase	(−) 1.4
Y00971	PRPS2; phosphoribosyl pyrophosphate synthetase 2	(−) 1.4
D78335	UMPK; uridine monophosphate kinase	(−) 1.3
J04031	MTHFD1; methylenetetrahydrofolate dehydrogenase	(−) 1.3
U31930	DUT; dUTP pyrophosphatase	(−) 1.3
Cell structure/adhesion		
X13839	ACTA2; actin, α2, smooth muscle, aorta	(+) 2.6
X01703	TUBA3; tubulin, α3	(+) 2.1
AB002313	PLXNB2; plexin B2	(+) 2.1
L25081	ARHC; ras hom. gene family, member C; RhoC	(+) 1.6
L05424	CD44; CD44 antigen (homing function)	(+) 1.5
M59040	CD44; CD44 antigen (homing function)	(+) 1.5
AB006782	LGALS9; lectin, galactoside-binding, soluble, 9 (galectin 9)	(+) 1.4
AF005392	TUBA2; tubulin, α2	(−) 1.3
U77718	PNN; pinin, desmosome-associated protein	(−) 1.3
Miscellaneous		
U53225	SNX1; sorting nexin 1	(+) 1.5
AB013924	LAMP3; lysosomal-associated membrane protein 3	(+) 2.4
M25629	KLK1; kallikrein 1, renal/pancreas/salivary	(+) 2.2
M29877	FUCA1; fucosidase, α-L-1, tissue	(+) 2.2
D11139	TIMP1; tissue inhibitor of metalloproteinase 1	(+) 2.1
X75593	RAB13; RAB13, member RAS oncogene family	(+) 2.0
AL050276	ZNF288; zinc finger protein 288	(+) 2.0
X79882	MVP; major vault protein	(+) 2.0
M92357	TNFAIP2; TNFα-induced protein 2	(+) 1.9
AB018549	MD-2; MD-2 protein; lymphocyte antigen 96	(+) 1.8
AF031815	KCNN3; K^+ intermediate/small conductance Ca-activated channel	(+) 1.8
X59871	TCF7; transcription factor 7 (T-cell specific, HMG-box)	(+) 1.7
U68019	MADH3; mothers against decapentaplegic hom. 3	(+) 1.7
AB029014	RAB6IP1; RAB6-interacting protein 1	(+) 1.7
M82809	ANXA4; annexin A4	(+) 1.6
AF039704	CLN2; ceroid-lipofuscinosis, neuronal 2, late infantile	(+) 1.6
Y08110	SORL1; sortilin-related receptor precursor	(+) 1.5
X85116	EPB72; erythrocyte membrane protein band 7.2	(+) 1.5
AL035306	STX12; syntaxin 12	(+) 1.5
AF039656	BASP1; brain abundant, membrane attached signal protein	(+) 1.5
U03985	NSF; *N*-ethylmaleimide-sensitive factor	(+) 1.5
AI671547	RAB9; RAB9, member RAS oncogene family	(+) 1.4
AF016903	AGRN; agrin	(+) 1.4
AA056747	ATP6A1; ATPase, H^+ transporting, lysosomal, α1	(+) 1.4
D49400	ATP6V1F; ATPase, H^+ transporting, lysosomal, V1F	(+) 1.3
M85169	PSCD1; pleckstrin homology, Sec7 and coiled/coil domain 1	(+) 1.3
AI741833	AP1G2; adaptor-related protein complex 1, γ2 subunit	(+) 1.3
X07743	PLEK; pleckstrin	(+) 1.3
AB018328	ALTE; Ac-like transposable element	(+) 1.3
M83822	LRBA; LPS-responsive vesicle trafficking, beach and anchor containing	(−) 2.3
AF036715	STX8; syntaxin 8	(−) 2.1
AB011113	WDR7; WD repeat domain 7	(−) 1.9
AF038660	B4GALT2; UDP-Gal:βGlcNAc:β1,4-galactosyltransferase	(−) 1.8
M80244	SLC7A5; solute carrier family 7 (cationic amino acid transporter)	(−) 1.6
D49489	P5; protein disulfide isomerase-related protein	(−) 1.6
U53347	SLC1A5; solute carrier family 1 (neutral amino acid transporter)	(−) 1.5
AF043250	TOMM40; translocase of outer mitochondrial membrane 40 hom.	(−) 1.5
U22055	p100; EBNA-2 co-activator (100 kDa)	(−) 1.5
AI262789	ERP70; protein disulfide isomerase related protein	(−) 1.5
AF059531	PRMT3; protein arginine *N*-methyltransferase 3	(−) 1.5
Y10805	HRMT1L2; hnRNP methyltransferase-like 2 (*S.cerevisiae*)	(−) 1.4
L17131	HMGA1; high-mobility group AT-hook 1	(−) 1.4
D32257	GTF3A; general transcription factor IIIA	(−) 1.4
AB028990	EXO70; likely ortholog of mouse exocyst protein hom.	(−) 1.4
AI660656	IGJ; immunoglobulin J chain	(−) 1.4
M63573	PPIB; peptidylprolyl isomerase B (cyclophilin B)	(−) 1.4

Table 2. *Continued*

Accession no.	Symbol; Name	*R*(*i*)
AJ011779	SEC63L; SEC63 protein	(−) 1.3
M22806	P4HB; procollagen-proline, 2-oxoglutarate 4-dioxygenase	(−) 1.3
Unknown		
AB022718	DEPP; decidual protein induced by progesterone	(+) 4.1
W27419	FLJ90005; hypothetical protein FLJ90005	(+) 2.6
AA149307	FLJ21174; hypothetical protein FLJ21174	(+) 1.6
AB023154	KIAA0937; KIAA0937 protein	(+) 1.6
Y13374	CXX1; CAAX box 1	(+) 1.6
AI800499	AIM1; absent in melanoma 1	(+) 1.5
AL049288	BLCAP; bladder cancer-associated protein	(+) 1.5
AL050190	DKFZP586B0923; DKFZP586B0923 protein	(+) 1.5
AF070539	MLF2; myeloid leukemia factor 2	(+) 1.4
D87434	KIAA0247; KIAA0247 gene product	(+) 1.4
D87446	RW1; likely ortholog of mouse Rw1	(+) 1.4
M68864	LOC51035; ORF	(+) 1.4
U90916	*H.sapiens* cDNA: FLJ21930 fis, clone HEP04301	(+) 1.4
AB011104	KIAA0532; KIAA0532 protein	(−) 3.0
AC002073	Unknown cDNA	(−) 1.5
AL050021	*H.sapiens* mRNA: cDNA from clone DKFZp564D016	(−) 1.5
D31887	KIAA0062; KIAA0062 protein	(−) 1.5
L19183	MAC30; hypothetical protein	(−) 1.5
M83751	ARMET; arginine-rich, mutated in early stage tumors	(−) 1.4

Abbreviations as in Table 1.
The 200 top-ranked probe sets by SAM with fold-changes greater than 1.3 were organized by functional category. Each gene was assigned to one category, as described in Figure 5. UV led to inducton of a majority of the 200 probe sets (60%).

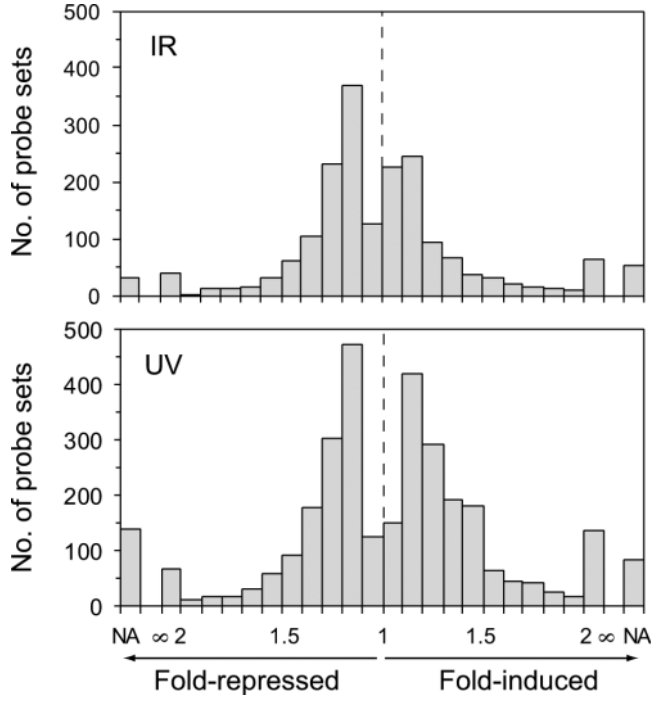

Figure 4. Distribution of fold-changes for damage-responsive probe sets. The histograms show the distribution of fold-changes for 1932 IR-responsive (upper panel) and 3143 UV-responsive (lower panel) probe sets, which were identified by SAM with an FDR of 10%. The bins between 2 and ∞ represent probe sets with more than 2-fold changes. The fold-change was not available (NA) for about 100 IR-responsive probe sets and 200 UV-responsive probe sets, because these probe sets had a negative value for expression either before or after exposure to DNA damage. Relatively few genes deemed significant by SAM had less than 1.1-fold responses even though 43 and 34% of the genes represented on the microarray had fold-changes in this range after IR and UV, respectively.

IR-responsive genes

Of the 200 top-ranked IR-responsive probe sets (Table 1), 56 were involved in cell cycle or cell proliferation. Two-thirds of these genes were repressed, including several cyclin genes (*A2*, *B1*, *B2* and *F*), cyclin-dependent kinase regulators (*CDC20*, *CKS2* and *CDKN3*), centromere genes (*CENPA*, *CENPE* and *CENPF*), mitotic kinesin-like genes (*KNSL1*, *KNSL2*, *KNSL5*, *KNSL6* and *KIF14*), mitosis-related kinases (*PLK*, *STK6*, *STK12*, *TTK* and *NEK2*) and proliferation genes (*myc*, *ASK* and *Ki-67*). IR induces a complex cascade of events leading to arrest of the cell cycle. For example, post-transcriptional phosphorylation of proteins that regulate the cell cycle occurs within minutes. However, cell cycle arrest must be maintained for many hours to permit the repair of DNA damage. Our microarray results reveal a coordinated dismantling of the cell cycle machinery by transcriptional repression, which may represent a mechanism for maintaining cell cycle arrest.

Among the cell cycle or proliferation genes that were induced, some were anti-proliferative (*TOB1*, *BTG1*, *BTG2* and *p21*), while others were growth-promoting (*granulin*, *CCNG1* and *PTP4A1*). These apparently paradoxical results may be due to the fact that the cells were grown asynchronously, and these opposing effects might occur in different subpopulations. Alternatively, cell-cycle checkpoints must be relieved to permit resumption of growth, and the observed responses may reflect both cell cycle arrest and preparation for reentry into the cell cycle in the same cell.

Of the 200 top-ranked probe sets, 18 probe sets representing 15 genes had roles in apoptosis, and all were induced. These included five members of the tumor necrosis factor (TNF)-receptor superfamily and genes that mediate p53-dependent apoptosis. Two of the fifteen genes were anti-apoptotic (*PEA15* and *DDR1*). Thus, as in the case of the cell cycle/

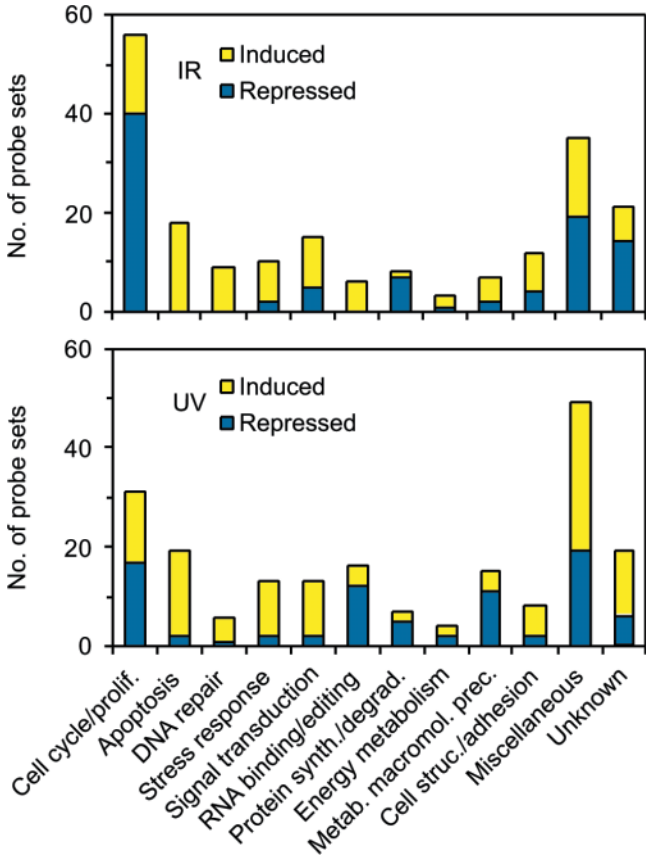

Figure 5. Functional categories of top-ranked damage-responsive genes. The 200 top-ranked IR-responsive probe sets (upper panel) and 200 top-ranked UV-responsive probe sets (lower panel) were categorized by function. The probe sets were identified by SAM with the additional criterion that the response to DNA damage was at least 1.3-fold in magnitude. Genes with more than one function were assigned to the more specific category. Thus, genes with anti-apoptotic functions were assigned to the 'Apoptosis' category, although they could have been assigned to the 'Cell cycle/proliferation' category. Genes in the 'DNA repair' category were not assigned to the 'Stress response' or 'Cell cycle/proliferation' categories. The highest specificity categories were 'DNA repair', 'Metabolism of macromolecular precursors' and 'Apoptosis'. 'Signal transduction' was considered to be the least specific category. For example, *MAPKAPK2* is involved in signal transduction, but was assigned to 'Stress response.'

proliferation genes, opposing effects were observed among the apoptosis genes.

Seven genes involved in DNA repair (corresponding to nine probe sets) were induced. *XPC*, *DDB2*, *PCNA* and *GADD45A* have roles in global genomic repair, a pathway for nucleotide excision repair of non-transcribed DNA. We previously discovered that these genes were induced following IR (19), suggesting that they may play a heretofore unrecognized role in the repair of IR-induced lesions. Also induced were *REV3L*, which encodes the catalytic subunit of the lesion bypass DNA polymerase zeta, and Ligase I (*LIG1*), which functions in base excision repair and DNA replication. In contrast, genes involved in other pathways for repairing IR-induced damage were not affected. IR-induced DNA double-strand breaks are repaired by homologous recombination or non-homologous end-joining. Although *RAD51C* was induced, many of the genes involved in homologous recombination (*XRCC2*, *XRCC3*, *MRE11*/*RAD50*/*NBS*, *BRCA1* and *BRCA2*) were unaffected by IR. Expression levels of genes involved in non-homologous end-joining (*Ligase IV*, *XRCC4*, *Ku80*, *Ku70* and *DNA-PK*) were also unchanged following IR. Many of the proteins encoded by these genes are regulated post-transcriptionally. For example, DNA-PK brings DNA ends together into a synaptic complex, and then undergoes activation of its kinase to phosphorylate target proteins (26). Alternatively, many DNA repair genes may have basal levels of expression sufficient for dealing with IR-induced damage.

Seven of the ten genes involved in the cellular stress response were induced. Some (*PIG3* and *GPX1*) deal with oxidative stress, while others encode proteins in the mitogen-activated protein kinase (MAPK) signaling pathway. Several transcription factor genes (*STAT3*, *ATF3*, *NFκB2* and *RELB*) were IR-induced, while *ETR101* was repressed. Two key genes that signal IR damage, *ATM* and *ATR*, showed only minor transcriptional responses.

Many genes had roles in G-protein signaling, which may activate adenylate cyclase to produce cAMP, or activate protein lipase C to produce inositol triphosphate and diacylglycerol. Genes involved in regulating G-proteins were either induced (*RGS16*) or repressed (*RBS19* and *GPRK5*). Induced genes were involved in phosphatidyl inositol signaling (*INPP1* and *PIK4CB*), diacylglycerol signaling (*DGKZ*) or cAMP signaling (*PRKX* and *PDE4B*). Thus, IR may produce a coordinated response in multiple components of G-protein signaling.

All five genes involved in RNA binding/editing were induced. The *APOBEC3C* and *APOBEC3G* genes are structurally and functionally related to the RNA-editing cytidine deaminase gene *APOBEC1*, which converts cytosine to uracil in apoB mRNA. Recently, these three genes were found to encode a DNA mutator activity, presumably inducing nucleotide substitutions at dC:dG in DNA (27). All three genes are homologous to *AID* (activation-induced cytidine deaminase), which converts cytosine to uracil at the immunoglobulin locus, triggering a pathway for somatic hypermutation. Our findings raise the possibility that IR induces a mutator phenotype at other loci targeted by the APOBEC proteins. Indeed, these proteins have distinct local target specificities. IR-induced mutators may promote rapid evolution of the survival of single cell organisms, but they may also amplify the carcinogenic effect of IR in humans.

The protein synthesis and degradation category was primarily composed of IR-repressed probe sets representing ubiquitin carrier or conjugating proteins. Some IR-responsive genes had functions related to energy metabolism, suggesting that cells cope with the effects of damage by altering energy production. Genes affecting the metabolism of macromolecular precursors were involved in the synthesis of nucleotides [thymidylate synthetase (*TYMS*)], fatty acids (*PRKAB1*) and tetrahydrobiopterin (*GCH1*), a cofactor required for the synthesis of aromatic amino acids. The induction of *TYMS* is notable, since the drug 5-fluorouracil, which inhibits TYMS, is often administered concurrently with radiation therapy to potentiate the anticancer activity of both agents. A group of 12 genes had roles in maintaining cell structure and regulating cell adhesion. Other genes had diverse functions, which included protein transport and targeting (*SEC14*, *TLOC1* and *fucosidase*), amino acid transport (*SLC1A1* and *SLC7A6*) and immune responsiveness (*MHC class I*, *PTPRCA* and *cytokine receptor-like factor 3*).

UV-responsive genes

Of the 200 top-ranked UV-responsive probe sets (Table 2), 31 were involved in cell cycle or proliferation. There was a considerable overlap between the IR- and UV-responsive genes in this category. Many genes induced by UV inhibit the cell cycle (*p21*, *TOB1*, *CCNG1*, *BTG1*, *RARRES*, *S100A11* and *RUNX3*), and many genes repressed by UV promote cell cycle progression (*MCM6*, *NOLC1*, *PTMA*, *DP1*, *DUSP5*, *POLA*, *POLE3*, *SRM*, *ODC* and *AMD1*).

Although 17 of the 19 top-ranked apoptosis probe sets were induced, many exert opposing effects. *BAX* and most of the TNF-related genes are pro-apoptotic, while *PEA15*, *DDR1*, *TRAF1*, *BIRC3*, *IER3* and *TAX1BP1* have anti-apoptotic effects.

Five DNA repair genes represented by six probe sets were responsive to UV. Four nucleotide excision repair genes were induced: *DDB2*, *XPC*, *GADD45* and *PCNA*. These global genomic repair genes were previously shown to be UV-induced, and were also IR-induced in this study, as discussed above. Other genes with roles in nucleotide excision repair included the transcription-coupled repair genes mutated in Cockayne syndrome, *CSA* and *CSB*. These genes were not ranked in the top 200 UV-responsive genes but were present among the genes with an FDR of 10%. Paradoxically, *CSA* was repressed 1.5-fold and *CSB* was induced 2.3-fold. This result may reflect an unrecognized role for CSB in dealing with UV damage after the completion of transcription-coupled repair. Another DNA repair gene, O6-methylguanine-DNA methyltransferase (*MGMT*), was repressed following UV. Inappropriate methylation of guanine to produce O6-methylguanine occurs spontaneously, independently of UV damage. However, the repression of *MGMT* would promote mutation of dG:dC to dA:dT after the resumption of DNA replication. Perhaps, this response enhances the mutator phenotype proposed above for the *APOBEC* genes. Several genes with key roles in nucleotide excision repair, including *XPA*, *XPD*, *XPG*, *DDB1* and *RPA*, did not have a biologically significant response, consistent with previous findings that these genes are not regulated transcriptionally.

Ten of the twelve stress response genes were induced by UV. These encoded transcription factors (*IRF5*, *NFκB2* and *ATF4*), quinone oxidoreductase homolog (*PIG3*), glutathione peroxidase (*GPX1*), the antioxidant protein 1 homolog (*ATOX1*) and heat-shock proteins (*HSPB1* and *HSPA1A*). Although not among the top-ranked 200 probe sets, *ATR* was slightly repressed by 1.15-fold following UV, while *ATM* was slightly induced by 1.17-fold.

Several signal transduction pathways contained UV-responsive genes. Genes involved in Ras or Rho signaling were responsive to UV (*DGKZ*, *ARHGDIA*, *TIP1*, *ARHC* and *PLXNB2*). Genes with immunological functions included receptors for IL4 (*IL4R*) and IL10 (*IL10RA*), as well as leupaxin (*LPXN*), which appears to be involved in a signaling pathway for focal adhesion of leukocytes (28).

RNA binding/editing genes induced by UV included three related genes (*APOBEC3C*, *APOBEC3G* and *APOBEC3B*). The first two genes were also induced by IR and have been shown to act as DNA mutators (27). Repressed genes included two related small nucleolar ribonucleoprotein genes involved in rRNA processing and modification (*NOLA2* and *DKC1*), and genes involved in RNA splicing (*SFRS2*, *NSAP1*, *HNRPAB* and *HNRPA3*).

Among the protein synthesis/degradation genes, UV exposure led to the suppression of five tRNA synthetases. UV produces damage to the 3′ end of 28S rRNA, leading to the inhibition of protein translation (29). Our results suggest that protein translation is also inhibited by repressed transcription of tRNA synthetase genes. The effects we observed were not a secondary effect of apoptosis, which is known to inhibit the initiation of protein synthesis [reviewed in (30)], since cell viability in our study at the time of cell harvesting was >90%. Other cellular stresses, including arsenite, hydrogen peroxide and sorbitol, have also been shown to cause profound inhibition of protein synthesis (31).

The UV response included many genes involved in the metabolism of macromolecular precursors. Significantly, nine genes were involved in nucleic acid metabolism. Genes with roles in pyrimidine (*DUT* and *UMPK*) and purine metabolism (*ADE2H*, *PFAS*, *PRPS2*, *AK2* and *ADK*) were repressed. Two genes with roles in nucleic acid degradation were induced. Adenosine deaminase (*ADA*) catalyzes hydrolysis of adenosine to inosine, and protein acid phosphatase 5 (*ACP5*) has a role in lysosomal catabolism of nucleotides (32). These responses lead to decreased synthesis and increased degradation of nucleic acids, which may protect the cell from incorporating damaged nucleotides into DNA.

Among the cell structure/adhesion genes, actin (*ACTA2*) and two actin-regulating genes (*ARHC* and *PLXNB2*) were induced by UV. Pinin, which may reinforce the intermediate filament–desmosome complex (33) was repressed by UV. Interestingly, two genes (*TUBA2* and *TUBA3*) encoding alpha tubulin showed opposite responses to UV, with possible effects on microtubule dynamics (34).

In the miscellaneous category, several UV-responsive genes had roles in various aspects of intracellular transport, including vesicle trafficking (*LRBA*, *AP1G2*, *NSF*, *STX12*, *RAB9*, *RAB13* and *RAB6IP1*), endo/exocytosis (*ANXA4* and *SORL1*), nucleocytoplasmic transport (*MVP*) and amino acid transport (*SLC1A5* and *SLC7A5*). All of these genes were induced except for the amino acid transport genes, *SLC1A5* and *SLC7A5*, and the vesicle trafficking gene, *LRBA*. One destination for vesicle traffic includes the lysosomes, and UV induced four genes with lysosomal functions (*SNX1*, *ATP6A1*, *ATP6V1F* and *LAMP3*). These responses may be a mechanism for disposing of proteins damaged by UV-induced cross-links.

Clustering of the top-ranked UV- and IR-responsive genes

The top-ranked UV- and IR-responsive genes and the 30 samples were organized by hierarchical clustering (Figure 6 and Supplementary Material Figure 1). As expected, the samples clustered strongly by the type of radiation used to treat the cells.

One prominent cluster of genes (Figure 6, red bar) contained 26 genes that were strongly repressed by IR, but not UV. Most of these genes were discussed above in terms of a coordinated dismantling of the cell cycle machinery after IR. The gene cluster included cyclin genes (*B1*, *B2* and *F*), cyclin-dependent kinase regulators (*CDC20* and *CKS2*), centromere genes (*CENPA*, *CENPE* and *CENPF*), mitotic kinesin-like genes

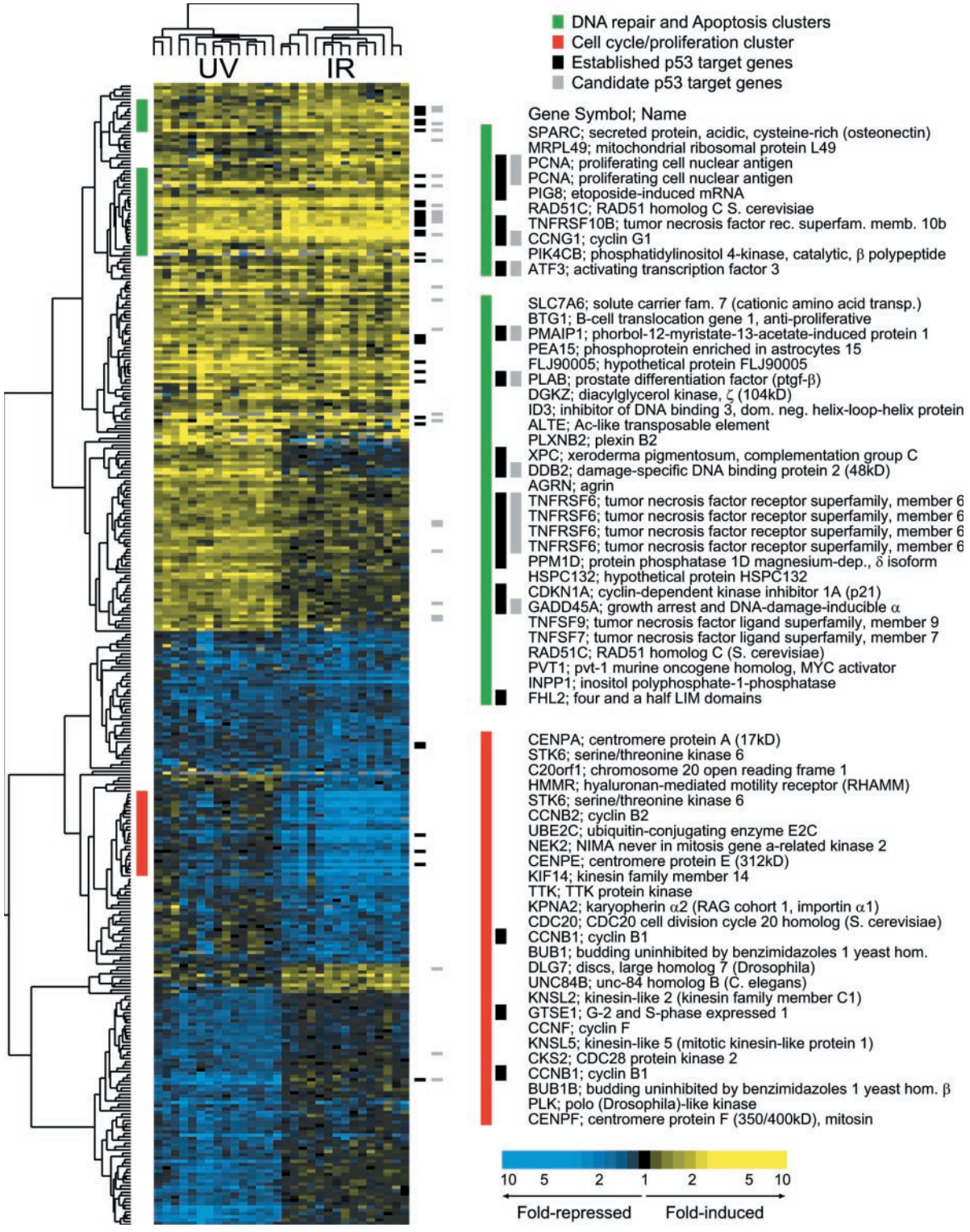

Figure 6. Hierarchical clustering of damage-responsive genes and samples. Data are shown for the top-ranked 200 UV-responsive probe sets and top-ranked 200 IR-responsive probe sets. The dendrogram to the left of the heat map shows clustering of the 350 probe sets (50 probe sets responded to both UV and IR). The dendrogram above the heat map shows clustering of the cell lines by treatment. The values used for clustering were the logarithm of the ratio of treatment (UV or IR) to mock treatment, and the scale to the lower right shows the fold-change indicated by each color. Yellow color represents induced expression following UV or IR, and blue color represents repressed expression. Gray spots on the heat map represent negative ratios of treatment to mock treatment for which logarithms values could not be computed. These cases occurred rarely and were generated because hybridization to the mismatched probes for that gene was greater than hybridization to the matched probes. There were 25 established p53-responsive genes, which are marked with a black bar to the right of the heat map. Four of these genes, *TNFRSF6*, *cyclin A2*, *cyclin B1* and *BAX*, were represented by two probe sets each, for a total of 29 probe sets. Putative p53-responsive genes are marked with a gray bar. The green bars indicate clusters that are enriched in genes involved in apoptosis and DNA repair. The red bar highlights a cluster that was strongly repressed by IR and enriched for genes involved in regulating the cell cycle and proliferation.

(*KNSL2*, *KNSL5* and *KIF14*) and mitosis-related kinases (*PLK*, *STK6*, *TTK* and *NEK2*). The cluster also included ubiquitin-conjugating enzyme E2 (*UBE2C*), which is required for the destruction of mitotic cyclins. This cluster is specifically repressed by IR and may reflect the fact that the double-strand breaks produced by IR pose a greater threat for mitotic catastrophe than lesions produced by UV. This threat may require a more extensive dismantling of the cell cycle machinery. Other genes in the cluster include hyaluronan-mediated motility receptor (*HMMR*, required for cell motility), karyopherin alpha 2 (*KPNA2*, involved in protein transport) and *UNC84B* (involved in nuclear migration). Their presence in this cluster raises the possibility that these genes have previously unrecognized roles in the cell cycle.

Genes induced after one or both forms of damage clustered at the top of the heat map. Two clusters are enriched in genes that function in DNA repair or apoptosis (Figure 6, green bars). The genes strongly induced by both UV and IR in the top one-third of the heat map are also enriched for genes known to respond to p53, consistent with the role of p53 in activating transcriptional responses to many forms of DNA damage. In fact, we identified about 90 established p53 target genes (represented by 142 probe sets) on the microarray, and almost one-third were ranked within the top 200 UV or IR-responsive genes (Figure 6, black bars). Moreover, almost half of the 142 probe sets were identified as significantly changed by SAM following UV or IR (FDR < 10%), and one-fourth were significantly changed by both UV and IR. Although UV or IR induced most of the p53-responsive genes, some of the genes were repressed, as was the case for *MGMT*, *cyclin A2*, *cyclin B1* and *cyclin F*.

We next used the UV and IR responses in this study to evaluate previous methods for identifying candidate p53 target genes. Hoh *et al*. (35) searched for candidate p53 target genes by employing an algorithm that searches for genes containing a consensus sequence for the p53 response element. Of the 308 highest-scoring genes with p53 response elements, 250 were represented on the microarray used in our study, and 108 were responsive to UV or IR (with an FDR = 10%). Kannan *et al*. (36) used microarrays to measure transcriptional responses in cells expressing a temperature-sensitive p53 protein. The cells were incubated with cyclohexamide to isolate primary p53 target genes. Of the 85 candidate p53 target genes identified by this method, 64 were represented on the microarray in our study, and 36 were responsive to UV or IR (with an FDR = 10%). Thus, approximately half of the candidate p53-responsive genes from both studies were responsive to UV or IR, and 25 genes were among the top-ranked 200 UV or IR-responsive probe sets (Figure 6, gray bars). Eleven of these genes were previously established as p53-responsive (Figure 6, black bars). Others clustered with established p53 genes and are therefore likely to be verified as bona fide p53-responsive genes.

Some candidate genes identified by Hoh *et al*. and Kannan *et al*. were not UV- or IR-responsive in our study. These genes may be regulated by p53 after other forms of damage or at other time points following damage. Also, some p53-responsive genes are regulated in a cell type-specific manner (35), and some genes may be silenced in lymphocytes. Finally, some of the genes identified by Hoh *et al*. may represent shortcomings of their algorithm, and some of the genes identified by Kannan *et al*. may represent nonphysiologic responses induced by artificial manipulation of the temperature-sensitive p53 gene.

The majority of the top-ranked genes in this study were not regulated by p53, particularly those repressed following DNA damage. Indeed, other transcription factors such as nuclear factor κB (NFκB) and activating protein-1 (AP-1) are involved in coordinating the cellular response to DNA damage. IR and UV both activate NFκB by inducing ubiquitin-dependent degradation of IκB, albeit by different pathways (37,38). Degradation of IκB releases NFκB for translocation for the cytoplasm to the nucleus. NFκB then induces the transcription of target genes with roles in immune responses, stress responses and cell survival [reviewed in (38)]. The top-ranked IR- and UV-responsive genes included two of the genes encoding NFκB itself (*NFκB2* and *RELB*) and two important NFκB target genes with functions in suppressing apoptosis, *TRAF1* (39) and *c-myc* (40).

The family of AP-1 transcription factors consists of dimeric proteins from the Jun, Fos, Maf and ATF subfamilies [reviewed in (41,42)]. UV activates AP-1 by a signaling pathway dependent on the c-Jun N-terminal kinase (JNK) and p38 MAPK cascades. IR activates AP-1 by a different pathway dependent on JNK and ATM (43). AP-1 regulates cellular responses involving proliferation, survival, apoptosis and differentiation. Although most of the target genes for AP-1 have not been identified, these responses suggest that the AP-1 target genes are represented among the IR- and UV-induced genes identified in this study.

In summary, the transcriptional responses to DNA damage in Figure 6 are due to the activation of several transcription factors, including p53, NFκB and AP-1. IR and UV activate each of these transcription factors by different mechanisms, perhaps accounting for differences between IR and UV in the kinetics of the transcriptional responses and in the identities of the responsive genes. The responses documented here represent the integrated effect of several transcription factors. For example, we observed a net induction of p21 transcription following UV or IR. This induction is known to be dependent on p53, but its magnitude was likely to be modulated by the repressive effect of AP-1 (42). Contributions from different transcription factors that respond in different ways to IR and UV may explain many of the distinctions between the IR and UV responses in Figure 6. These contributions may generate the clusters of genes that were induced or repressed by both agents, or induced or repressed by one agent but not the other.

DISCUSSION

This study presents a portrait of the transcriptional responses to UV and IR in human cells. The study employed microarrays containing probes for an estimated one-third of the genes in the genome, and used cells derived from 15 individuals, a far greater number than were used in previous studies. Analysis of such a large number of samples permitted identification of a large number of responsive genes and ensured that our results were not subject to genetic defects or polymorphisms from any single individual. A robust statistical method, SAM, identified responsive genes and established the accuracy of its results by estimating an FDR. The genes were further validated by northern blots and independent microarray experiments. Finally,

many of the genes identified by SAM were previously identified by conventional laboratory methods. Thus, the damage response defined by this study has been subjected to a rigorous assessment of its validity to a degree not achieved by earlier studies.

Having established the validity of our data, we felt justified in reaching several significant conclusions. One-third of the genes on the microarray were responsive to UV and one-fourth of the genes were responsive to IR. These are very large fractions, but still may be underestimates, since individual genes respond with different time courses or to different doses of radiation. Additionally, transcriptional responses to damage vary widely in different cell lines and cell types (44). Furthermore, the analysis of an even larger number of cell lines would yield improved FDRs and permit the identification of even more responsive genes. Although a large fraction of the genome was responsive to DNA damaging agents, only a few hundred genes exhibited responses as large as 2-fold.

Do these transcriptional responses produce protein responses? Although a global proteomic analysis is beyond the scope of this study, there is evidence that changes in transcription lead to changes in the levels of the proteins that produce biological effects. Mootha *et al*. (45) obtained proteomic and gene expression data in mitochondria from different mouse tissues and found concordance between mRNA and protein levels in 426 of 569 pairwise comparisons. Thus, mRNA levels correlate strongly with protein levels.

Of the 200 top-ranked damage-responsive genes, 59% had unexpected functions not previously associated with the IR or UV response. Large groups of genes had functions in signal transduction, RNA binding and editing, protein synthesis and degradation, energy metabolism, metabolism of macromolecular precursors, and cell structure and adhesion. Many genes had miscellaneous functions, including vesicle transport, amino acid transport, lysosomal metabolism, transcriptional regulation and immune function. Several genes with a mutator phenotype were induced, possibly amplifying the carcinogenic effects of DNA damaging agents.

About 41% of responsive genes could be assigned to functional categories that might have been anticipated a priori. These functional categories were cell cycle and proliferation, apoptosis, DNA repair and the stress response. Nevertheless, there were unexpected results within the categories. Arrest of the cell cycle, particularly after IR, appeared to include a coordinated transcriptional repression of many components of the cell cycle machinery, providing what may be an important mechanism for maintaining the cell cycle arrest initiated by the more extensively studied phosphorylation pathways. Induction of DNA repair genes after IR was notable for genes previously associated with the repair of UV-induced damage, not IR-induced damage.

Transcriptional responses to DNA damage do not necessarily promote survival of the cell. In yeast, a deletion strain has been created for every gene in the genome, permitting the identification of genes that affect survival after exposure to DNA damaging agents. These genes correlate weakly with the genes that respond transcriptionally to the same DNA damaging agents (46). Indeed, some responses that we observed in human cells were pro-apoptotic. Other responses involved genes with physiological effects that are likely to be unrelated to survival of the individual cell.

It is instructive to compare the damage responses in humans and yeast. Gasch *et al*. (47) measured transcriptional responses in yeast after exposure to 170 Gy IR at eight time points over 2 h. Although they used a much higher IR dose than we used for human cells, viability of the yeast remained greater than 45%, as expected from the much smaller size of the yeast genome. Extensive changes in transcription occurred across the entire yeast genome. In fact, 1300 of 6200 transcripts changed by more than 2-fold. The percentage of robust changes was much higher than we found for human cells, perhaps because the yeast cells were exposed to a much higher IR dose. However, we found a large number of human genes, which may produce physiological effects comparable to the yeast responses.

Gasch *et al*. (47) provided supplementary data, allowing us to confirm that the transcriptional responses in yeast and humans were similar in many respects. As we have discovered in humans, the IR response in yeast included many cell cycle regulation genes, but few DNA repair genes. The yeast and human responses also involved several unexpected pathways that were noted above. These included pathways for protein synthesis and degradation, metabolite transport, carbohydrate metabolism and metabolism of various macromolecular precursors, including purines, pyrimidines and amino acids. Although the physiological role of these responses is currently obscure, they are conserved from yeast to humans.

On the other hand, the yeast and human responses included notable differences, usually in pathways that were not present in both organisms. The yeast IR response included genes involved in cell wall biogenesis, a biochemical pathway not present in humans. Conversely, the human response included genes involved in apoptosis, cell adhesion, intracellular transport and immunity, many of which are absent or less complex in yeast.

It is important to note the limitations of this study. Transcriptional responses to damage can vary in different cell types and at different radiation doses or time points following radiation. In this study, we characterized the responses in a single cell type, at a single time point, and at a single radiation dose. Additionally, altered transcript levels could result from changes in transcription or from changes in transcript degradation. Furthermore, the responses to DNA damage include both primary and secondary responses. To address all of these limitations, future experiments must employ very large numbers of microarrays, which are beyond the scope of this study. Nevertheless, our portrait of the transcriptional response to DNA damage is more complete than previous studies on human cells.

Another limitation is that the transcriptional responses reported here are relative to the responses of all other genes in the genome. The data from each microarray were scaled against the average of all other microarrays in the study. Because of data scaling, we cannot detect global decreases in transcription following damage. Previous studies have reported global inhibition of transcription following UV (48) and IR (49). This reduced transcription following UV is linked to transcription-coupled repair, a major pathway for nucleotide excision repair of UV-induced damage. It is also linked to ubiquitination and degradation of RNA polymerase II.

Finally, our study utilized lymphoblastoid cell lines, which are B-lymphocytes immortalized by Epstein–Barr virus. The

process of immortalization produces 2-fold changes in the transcription of only 1% of all genes (50). Moreover, we were able to confirm that the transcriptional responses reported here also occurred in peripheral blood lymphocytes. Primary lymphocytes from seven individuals were induced to enter the cell cycle with T-cell mitogens, treated with 5 Gy IR as in this paper, and analyzed 4 h later for transcriptional responses with the Affymetrix U133 GeneChip (R. Kimura, C. Kirk, K. Rieger, G. Chu, V. Stanton, D. Chasman and C. Hoban, unpublished data). Despite a different cohort of individuals, different cell types and different microarray platforms, 83% of the responses in Table 2 that were 2-fold or larger were also observed in primary lymphocytes.

We chose to use lymphoblastoid cell lines for several reasons. First, in contrast to resting B cells, lymphoblastoid cells proliferate in culture, permitting us to study the responses of cell cycle genes. Second, our data focus on changes in expression after DNA damage, and alterations due to immortalization that are confined to basal levels of gene expression will not affect our results. Third, our analysis of the damage response in normal human lymphoblastoid cells provides a reference point for future studies employing the large number of mutant lymphoblastoid cell lines that already exist. Indeed, cellular phenotypes have been established in lymphoblastoid cell lines representing several inherited defects in the DNA damage response, including xeroderma pigmentosum, Cockayne syndrome, ataxia telangiectasia and Fanconi anemia (2).

In summary, the human transcriptional response to DNA damage was more complex than previously recognized. Many of the responses may represent transcriptional programs with effects on the cell that are distinct from its survival. Most of the genes identified here belonged to unanticipated biochemical pathways, altering the conventional view of how human cells respond to DNA damage. This portrait of the damage response provides a foundation for future studies.

SUPPLEMENTARY MATERIAL

Supplementary Material is available at NAR Online.

ACKNOWLEDGEMENTS

We thank J. Budman, B. Ekstrand, L. DeFazio, W. J. Hong, S. Kim, J. Rusmintratip, L. Sacks and T. Tan for reading the manuscript, J. Tang, R. Tibshirani and V. G. Tusher for helpful discussions, and A. Chu for help in analyzing the primary lymphocyte data. This work was supported by funding from the Medical Scientist Training Program to K.E.R. and a Burroughs-Wellcome Clinical Scientist Award for Translational Research to G.C.

REFERENCES

1. Holbrook,N.J., Liu,Y. and Fornace,A.J.,Jr (1996) Signaling events controlling the molecular response to genotoxic stress. In Feige,U., Morimoto,R.I., Yahara,I. and Polla,B.S. (eds), *Stress-Inducible Cellular Responses.* Birkhauser/Springer, Vol. 77, pp. 273–288.
2. Friedberg,E.C., Walker,G.C. and Siede,W. (1995) *DNA Repair and Mutagenesis.* ASM Press, Washington, DC.
3. Nickoloff,J.A. and Hoekstra,M.F. (1998) *DNA Damage and Repair*. Humana Press, Totowa, NJ.
4. Birrell,G.W., Giaever,G., Chu,A.M., Davis,R.W. and Brown,J.M. (2001) A genome-wide screen in *Saccharomyces cerevisiae* for genes affecting UV radiation sensitivity. *Proc. Natl Acad. Sci. USA*, **98**, 12608–12613.
5. Mercier,G., Denis,Y., Marc,P., Picard,L. and Dutreix,M. (2001) Transcriptional induction of repair genes during slowing of replication in irradiated *Saccharomyces cerevisiae*. *Mutat. Res.*, **487**, 157–172.
6. Gasch,A., Spellman,P., Kao,C., Carmel-Harel,O., Eisen,M., Storz,G., Botstein,D. and Brown,P. (2000) Genomic expression programs in the response of yeast cells to environmental changes. *Mol. Biol. Cell*, **11**, 4241–4257.
7. Chen,D., Toone,W.M., Mata,J., Lyne,R., Burns,G., Kivinen,K., Brazma,A., Jones,N. and Bahler,J. (2003) Global transcriptional responses of fission yeast to environmental stress. *Mol. Biol. Cell*, **14**, 214–229.
8. Courcelle,J., Khodursky,A., Peter,B., Brown,P.O. and Hanawalt,P.C. (2001) Comparative gene expression profiles following UV exposure in wild-type and SOS-deficient *Escherichia coli*. *Genetics*, **158**, 41–64.
9. Cromie,G.A., Connelly,J.C. and Leach,D.R. (2001) Recombination at double-strand breaks and DNA ends: conserved mechanisms from phage to humans. *Mol. Cell*, **8**, 1163–1174.
10. Bentley,N.J. and Carr,A.M. (1997) DNA structure-dependent checkpoints in model systems. *Biol. Chem.*, **378**, 1267–1274.
11. Sesto,A., Navarro,M., Burslem,F. and Jorcano,J.L. (2002) Analysis of the ultraviolet B response in primary human keratinocytes using oligonucleotide microarrays. *Proc. Natl Acad. Sci. USA*, **99**, 2965–2970.
12. Li,L., Story,M. and Legerski,R.J. (2001) Cellular responses to ionizing radiation damage. *Int. J. Radiat. Oncol. Biol. Phys.*, **49**, 1157–1162.
13. Park,W.Y., Hwang,C.I., Im,C.N., Kang,M.J., Woo,J.H., Kim,J.H., Kim,Y.S., Kim,H., Kim,K.A., Yu,H.J. *et al.* (2002) Identification of radiation-specific responses from gene expression profile. *Oncogene*, **21**, 8521–8528.
14. Guo,Y.L., Chang,H.C., Tsai,J.H., Huang,J.C., Li,C., Young,K.C., Wu,L.W., Lai,M.D., Liu,H.S. and Huang,W. (2002) Two UVC-induced stress response pathways in HeLa cells identified by cDNA microarray. *Environ. Mol. Mutagen.*, **40**, 122–128.
15. Ford,B.N., Wilkinson,D., Thorleifson,E.M. and Tracy,B.L. (2001) Gene expression responses in lymphoblastoid cells after radiation exposure. *Radiat. Res.*, **156**, 668–671.
16. Li,D., Turi,T.G., Schuck,A., Freedberg,I.M., Khitrov,G. and Blumenberg,M. (2001) Rays and arrays: the transcriptional program in the response of human epidermal keratinocytes to UVB illumination. *FASEB J.*, **15**, 2533–2535.
17. Murakami,T., Fujimoto,M., Ohtsuki,M. and Nakagawa,H. (2001) Expression profiling of cancer-related genes in human keratinocytes following non-lethal ultraviolet B irradiation. *J. Dermatol. Sci.*, **27**, 121–129.
18. Becker,B., Vogt,T., Landthaler,M. and Stolz,W. (2001) Detection of differentially regulated genes in keratinocytes by cDNA array hybridization: Hsp27 and other novel players in response to artificial ultraviolet radiation. *J. Invest. Dermatol.*, **116**, 983–988.
19. Tusher,V., Tibshirani,R. and Chu,G. (2001) Significance analysis of microarrays applied to the ionizing radiation response. *Proc. Natl Acad. Sci. USA*, **98**, 5116–5121.
20. Rieger,K.E., Hong,W.J., Tusher,V.G., Tang,J., Tibshirani,R. and Chu,G. (2004) Toxicity from radiation therapy associated with abnormal transcriptional responses to DNA damage. *Proc. Natl Acad. Sci. USA*, **101**, 6635–6640.
21. Eisen,M., Spellman,P., Brown,P. and Botstein,D. (1998) Cluster analysis and display of genome-wide expression patterns. *Proc. Natl Acad. Sci. USA*, **95**, 14863–14868.
22. Boothman,D., Bouvard,I. and Hughes,E. (1989) Identification and characterization of X-ray-induced proteins in human cells. *Cancer Res.*, **49**, 2871–2878.
23. Lu,X. and Lane,D.P. (1993) Differential induction of transcriptionally active p53 following UV or ionizing radiation: defects in chromosome instability syndromes? *Cell*, **75**, 765–778.
24. Blattner,C., Kannouche,P., Litfin,M., Bender,K., Rahmsdorf,H.J., Angulo,J.F. and Herrlich,P. (2000) UV-induced stabilization of c-fos and other short-lived mRNAs. *Mol. Cell. Biol.*, **20**, 3616–3625.
25. Storey,J. (2002) A direct approach to false discovery rates. *J. R. Stat. Soc. B*, **64**, 479–498.

26. DeFazio,L., Stansel,R., Griffith,J. and Chu,G. (2002) Synapsis of DNA ends by the DNA-dependent protein kinase. *EMBO J.*, **21**, 3192–3200.
27. Harris,R.S., Petersen-Mahrt,S.K. and Neuberger,M.S. (2002) RNA editing enzyme APOBEC1 and some of its homologs can act as DNA mutators. *Mol. Cell*, **10**, 1247–1253.
28. Lipsky,B.P., Beals,C.R. and Staunton,D.E. (1998) Leupaxin is a novel LIM domain protein that forms a complex with PYK2. *J. Biol. Chem.*, **273**, 11709–11713.
29. Iordanov,M.S., Pribnow,D., Magun,J.L., Dinh,T.H., Pearson,J.A. and Magun,B.E. (1998) Ultraviolet radiation triggers the ribotoxic stress response in mammalian cells. *J. Biol. Chem.*, **273**, 15794–15803.
30. Clemens,M.J., Bushell,M., Jeffrey,I.W., Pain,V.M. and Morley,S.J. (2000) Translation initiation factor modifications and the regulation of protein synthesis in apoptotic cells. *Cell Death Differ.*, **7**, 603–615.
31. Patel,J., McLeod,L.E., Vries,R.G., Flynn,A., Wang,X. and Proud,C.G. (2002) Cellular stresses profoundly inhibit protein synthesis and modulate the states of phosphorylation of multiple translation factors. *Eur. J. Biochem.*, **269**, 3076–3085.
32. Suter,A., Everts,V., Boyde,A., Jones,S.J., Lullmann-Rauch,R., Hartmann,D., Hayman,A.R., Cox,T.M., Evans,M.J., Meister,T. *et al.* (2001) Overlapping functions of lysosomal acid phosphatase (LAP) and tartrate-resistant acid phosphatase (Acp5) revealed by doubly deficient mice. *Development*, **128**, 4899–4910.
33. Shi,J. and Sugrue,S.P. (2000) Dissection of protein linkage between keratins and pinin, a protein with dual location at desmosome-intermediate filament complex and in the nucleus. *J. Biol. Chem.*, **275**, 14910–14915.
34. Bode,C., Gupta,M., Suprenant,K. and Himes,R. (1993) The two alpha-tubulin isotypes in budding yeast have opposing effects on microtubule dynamics *in vitro*. *EMBO Rep.*, **4**, 94–99.
35. Hoh,J., Jin,S., Parrado,T., Edington,J., Levine,A.J. and Ott,J. (2002) The p53MH algorithm and its application in detecting p53-responsive genes. *Proc. Natl Acad. Sci. USA*, **99**, 8467–8472.
36. Kannan,K., Amariglio,N., Rechavi,G., Jakob-Hirsch,J., Kela,I., Kaminski,N., Getz,G., Domany,E. and Givol,D. (2001) DNA microarrays identification of primary and secondary target genes regulated by p53. *Oncogene*, **20**, 2225–2234.
37. Li,N. and Karin,M. (1998) Ionizing radiation and short wavelength UV activate NF-kappaB through two distinct mechanisms. *Proc. Natl Acad. Sci. USA*, **95**, 13012–13017.
38. Li,X. and Stark,G.R. (2002) NFkappaB-dependent signaling pathways. *Exp. Hematol.*, **30**, 285–296.
39. Wang,C.Y., Mayo,M.W., Korneluk,R.G., Goeddel,D.V. and Baldwin,A.S.,Jr (1998) NF-kappaB antiapoptosis: induction of TRAF1 and TRAF2 and c-IAP1 and c-IAP2 to suppress caspase-8 activation. *Science*, **281**, 1680–1683.
40. Wu,M., Arsura,M., Bellas,R.E., FitzGerald,M.J., Lee,H., Schauer,S.L., Sherr,D.H. and Sonenshein,G.E. (1996) Inhibition of c-myc expression induces apoptosis of WEHI 231 murine B cells. *Mol. Cell. Biol.*, **16**, 5015–5025.
41. Shaulian,E. and Karin,M. (2001) AP-1 in cell proliferation and survival. *Oncogene*, **20**, 2390–2400.
42. Shaulian,E. and Karin,M. (2002) AP-1 as a regulator of cell life and death. *Nature Cell Biol.*, **4**, E131–136.
43. Lee,S.A., Dritschilo,A. and Jung,M. (1998) Impaired ionizing radiation-induced activation of a nuclear signal essential for phosphorylation of c-Jun by dually phosphorylated c-Jun amino-terminal kinases in ataxia telangiectasia fibroblasts. *J. Biol. Chem.*, **273**, 32889–32894.
44. Amundson,S.A., Bittner,M., Chen,Y., Trent,J., Meltzer,P. and Fornace,A.J.,Jr (1999) Fluorescent cDNA microarray hybridization reveals complexity and heterogeneity of cellular genotoxic stress responses. *Oncogene*, **18**, 3666–3672.
45. Mootha,V.K., Bunkenborg,J., Olsen,J.V., Hjerrild,M., Wisniewski,J.R., Stahl,E., Bolouri,M.S., Ray,H.N., Sihag,S., Kamal,M. *et al.* (2003) Integrated analysis of protein composition, tissue diversity, and gene regulation in mouse mitochondria. *Cell*, **115**, 629–640.
46. Birrell,G.W., Brown,J.A., Wu,H.I., Giaever,G., Chu,A.M., Davis,R.W. and Brown,J.M. (2002) Transcriptional response of *Saccharomyces cerevisiae* to DNA-damaging agents does not identify the genes that protect against these agents. *Proc. Natl Acad. Sci. USA*, **99**, 8778–8783.
47. Gasch,A.P., Huang,M., Metzner,S., Botstein,D., Elledge,S.J. and Brown,P.O. (2001) Genomic expression responses to DNA-damaging agents and the regulatory role of the yeast ATR homolog Mec1p. *Mol. Biol. Cell*, **12**, 2987–3003.
48. Takeda,S., Naruse,S. and Yatani,R. (1967) Effects of ultra-violet microbeam irradiation of various sites of HeLa cells on the synthesis of RNA, DNA and protein. *Nature*, **213**, 696–697.
49. Luchnik,A.N., Hisamutdinov,T.A. and Georgiev,G.P. (1988) Inhibition of transcription in eukaryotic cells by X-irradiation: relation to the loss of topological constraint in closed DNA loops. *Nucleic Acids Res.*, **16**, 5175–5190.
50. Carter,K.L., Cahir-McFarland,E. and Kieff,E. (2002) Epstein–Barr virus-induced changes in B-lymphocyte gene expression. *J. Virol.*, **76**, 10427–10436.